TECHNISCHE UNIVERSITÄT WIEN

Diploma Thesis

Synthesis of Nitrogen-Incorporated Indolo[3,2,1-*jk*]carbazole Derivatives

conducted at the

Institute of Applied Synthetic Chemistry

at the **TU Wien**

under the supervision of

Univ.Prof. Dipl. -Ing. Dr.techn. Johannes **Fröhlich**

advised by

Dipl. -Ing. Dr.techn. Paul **Kautny**

and

Dipl. -Ing. Dr.techn. Thomas **Kader**

by

Birgit **Meindl**, BSc.

Matr.-Nr.: 01126399

Humboldtgasse 28/19, 1100 Wien

Vienna, March 2020

Danksagung

Als Erstes möchte ich mich bei Herrn Prof. **Johannes Fröhlich** bedanken, der mir die Möglichkeit gegeben hat, meine Diplomarbeit in seiner Forschungsgruppe auszuführen.

Ein großes Danke an meine beiden Betreuer Dr. **Paul Kautny** und Dr. **Thomas Kader**, die diese Forschungsarbeit möglich machten. Besonders danke ich Dr. Thomas Kader für die direkte Betreuung im Labor und für die zahlreichen Hilfestellungen sowohl bei praktischen Arbeiten als auch für theoretische Hintergründe.

Weiters möchte ich mich bei Dr. **Brigitte Holzer** herzlich für die Hilfestellung bei diversen Problemen und Messung und Auswertung von NMR-Proben bedanken. Auch Dr. **Christian Hametner** bin ich sehr dankbar für zahlreiche NMR-Messungen und Hilfestellung bei komplizierteren Spektren.

Ich bedanke mich bei meinen Laborkollegen DI **Dorian Bader**, Dr. **Brigitte Holzer**, DI **Nikolaus Poremba** und **Paul Getreuer** für das angenehme und lustige Arbeitsklima, für die gute Zusammenarbeit und für die lustigen Freizeitaktivitäten. Auch bei Dr. **Florian Glöcklhofer** möchte ich mich bedanken, der mich durch die Betreuung meiner Bachelorarbeit in die Arbeitsgruppe gebracht und mir viele wertvolle Skills im synthetischen Labor beigebracht hat.

Ein besonderer Dank gilt meinen Eltern **Klaus** und **Regina Meindl**, die mich in den letzten 26 Jahren unterstützt haben und ohne denen dieses Studium nicht möglich gewesen wäre. Danke für die emotionale und finanzielle Unterstützung während dieser Zeit. Auch bei meinen Großeltern **Friedrich** und **Erika Meindl** möchte ich mich für die Unterstützung bedanken.

Ich möchte mich bei meinen Freunden **Kristina Hager**, **Lena Zanghellini**, **Hannah Kastinger**, **Laura Stix**, **Alina Heizinger**, **Katharina Edlinger**, **Tamara De Zuani** und **Pia Hochreiner** bedanken, auf die ich in guten als auch in schwierigen Zeiten immer zählen konnte.

Als letztes möchte ich meinem Freund **Dorian Bader** danken, der mich sowohl bei fachlichen Fragestellungen als auch emotional sehr unterstützt hat und in schwierigen Zeiten hinter mir gestanden ist.

Abstract

In the last decades a lot of research was focused on the field of organic electronics, especially on organic light emitting diodes (OLEDs). Organic materials based on π-conjugated small molecules, like triphenylamine or anthracene derivatives are commonly used in OLED applications like smartphone displays or TV screens.

The development of phosphorescent OLEDs (PhOLEDs) overcame the limitation of fluorescent based devices, which could only harvest singlet excitons and therefore were limited by 25% internal quantum yield. PhOLEDs can use both singlet and triplet excitons through intersystem crossing and therefore reach theoretically 100% internal quantum efficiency.

To prevent quenching effects triggered by a high concentration of triplet excitons, host materials are required in PhOLED devices, which must fulfill certain criteria, for example suitable HOMO/LUMO levels and balanced charge transport properties, which is realized by bipolar host materials.

Our research group recently introduced indolo[3,2,1-*jk*]carbazole (ICz) as donor moiety in bipolar host materials. With increased planarization from triphenylamine to phenylcarbazole and ICz the donor strength decreases to the point where also weak acceptor properties were observed for ICz. To further increase the acceptor strength, electron-withdrawing pyridine-like nitrogen atoms were incorporated into the ICz scaffold (NICz).

It was observed that incorporation of pyridine-like nitrogen into the ICz scaffold lowers the energy of HOMO and LUMO compared to ICz. Additionally, this study unveiled that both amount and position of the nitrogen atoms influences photophysical and electrochemical properties. Also, changing the position of the nitrogen atoms leads to different orientation and packing in the crystalline state due to non-classical C-H···N hydrogen bonds.

With this knowledge in mind, the main focus of this thesis was to incorporate the NICz scaffold into larger conjugated systems. Furthermore, alternative strategies towards different NICzs together with a new NICz building block, which was previously not investigated, were targets of this work. Special focus of this thesis was the investigation and evaluation of different synthetic strategies towards these systems. The insight on the practicability of the strategies represents a helpful tool for the design of other NICzs or similar systems. The effect of the introduction of nitrogen atoms on the materials properties should be compared to the previous results.

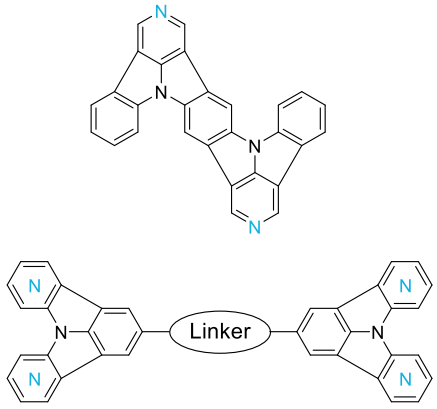

Incorporation of NICz in larger systems

Kurzfassung

In den letzten Jahren wurde intensive Forschung in der organischen Elektronik betrieben, insbesondere in der Entwicklung von organischen Leuchtdioden (OLEDs). Organische Materialien basierend auf π-konjugierten Systemen, wie zum Beispiel Triphenylamin oder Anthracen Derivaten, werden in OLEDs für Smartphone-Displays oder Fernseher bereits eingesetzt.

Mit der Entwicklung von OLEDs basierend auf Phosphoreszenz (PhOLEDs), die im Vergleich zu fluoreszierenden OLEDs sowohl Singulett- als auch Triplett-Exzitons zur Emission verwenden und somit theoretisch eine interne Quantenausbeute von 100% erreichen können, sind besonders effiziente Devices möglich.

Um Quenching Effekte zu verhindern, die durch eine hohe Konzentration von Triplett-Exzitons hervorgerufen werden, müssen die Emitter in ein Hostmaterial eingebettet werden. Für effiziente OLED Devices müssen Hostmaterialien bestimmte Anforderungen erfüllen, wie passende HOMO/LUMO Levels und ein ausgeglichener Ladungstransport, was durch bipolare Hostmaterialien erreicht wird.

Indolo[3,2,1-*jk*]carbazol (ICz) wurde in unserer Arbeitsgruppe als Donor-Einheit für bipolare Hostmaterialien eingeführt. Durch die Planarisierung von Triphenylamin zu Phenylcarbazol und ICz konnte die Donorstärke gesenkt werden. Für ICz wurden auch schwache Akzeptor-Eigenschaften beobachtet, die durch den Einbau von Stickstoff-Atomen in den ICz-Baustein (NICz) verstärkt werden konnten.

Durch den Stickstoffeinbau wurde im Vergleich zu ICz eine Erniedrigung der HOMO und LUMO Energielevels erreicht. Zusätzlich wurde herausgefunden, dass die Stickstoffposition und -anzahl die photophysikalischen und elektrochemischen Eigenschaften sowie, aufgrund nicht-klassischer C-H···N Wasserstoffbrücken, die Kristallpackung beeinflusst.

Der Fokus dieser Arbeit lag beim Einbau von NICz-Einheiten in größere, konjugierte Systeme. Zusätzlich sollten alternative Syntheserouten für verschieden NICzs und auch ein neuer NICz-Baustein entwickelt werden. Das Hauptziel war die Entwicklung und Evaluierung verschiedener, synthetischer Strategien. Die Erfahrungen der Anwendbarkeit der Synthesen bringt Nutzen für die Entwicklung anderer NICzs oder ähnlichen Systemen. Die durch den Stickstoffeinbau hervorgerufenen Effekte sollen mit den vorherigen Ergebnissen verglichen werden.

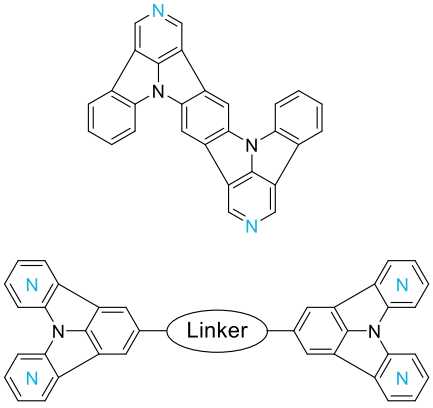

Schematische Darstellung der Zielmoleküle

Abbreviation

ACN	acetonitrile
AcOH	acetic acid
BHA	Buchwald-Hartwig Amination
CHA	CH Activation
dba	dibenzylideneacetone
DCM	dichloromethane
DMA	*N,N*-dimethylacetamide
DME	dimethylether
DMF	*N,N*-dimethylformamide
DMSO	dimethylsulfoxide
dppf	1,1´-bis(diphenylphosphino)ferrocene
EE	ethyl acetate
eq	equivalents
EtOH	ethanol
GC	gas chromatography
iPrOH	isopropanol
LP	light petroleum
MeOH	methanol
MS	mass spectrometry
nBuLi	*n*-butyl lithium
NCS	*N*-chlorosuccinimide
NMP	*N*-methyl-2-pyrrolidon
NMR	nuclear magnetic resonance
rac-BINAP	racemic 2,2′-bis(diphenylphosphino)-1,1′-binaphthalene
rt	room temperature
SG	silica gel
S_N	nucleophilic substitution
T	temperature
TEOF	triethyl orthoformate
THF	tetrahydrofuran
TMS	trimethylsilyl

General Remarks

Labeling of substances

Identification of substances was achieved by strict sequential numbering. Substances previously reported in literature receive Arabic numbers, whereas substances unknown to literature are labeled with Roman numbers.

References to literature citations

References to literature are given within the text by superscript Arabic numbers in square brackets.

Nomenclature

The nomenclature of chemical compounds not described in literature was based on the rules of Chemical Abstracts. Other compounds, reagents and solvents may be described by simplified terms, trivial or trade names.

Table of Contents

A. Formula Scheme

A.1 Target Molecule TM1

A.1.1 The Bromo-carboline Approach

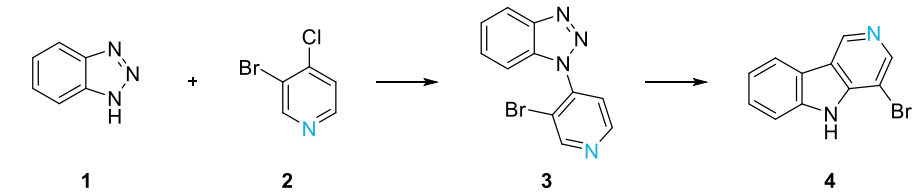

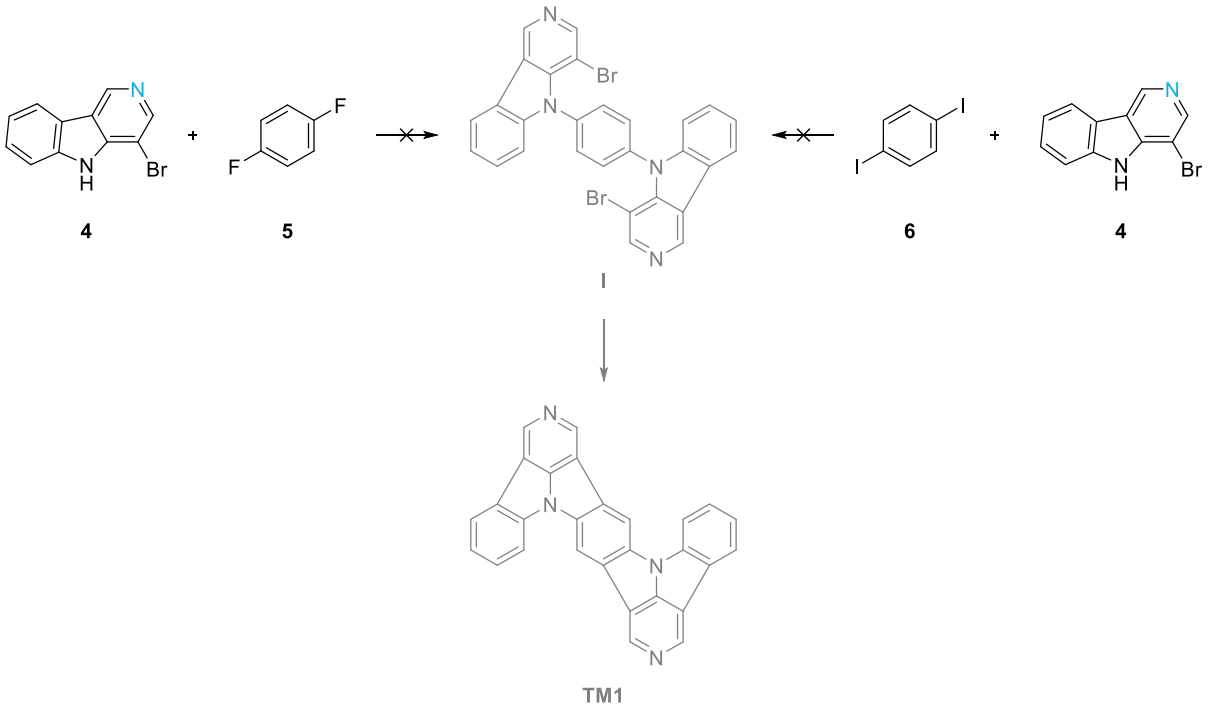

A.1.2 The Di(chloro-carboline) Approach

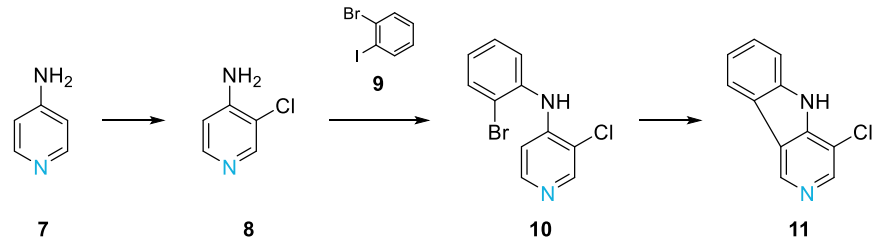

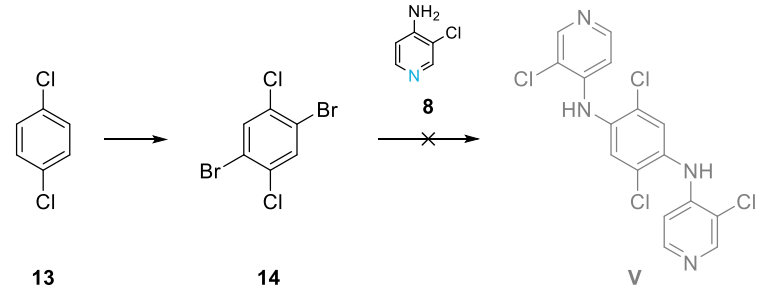

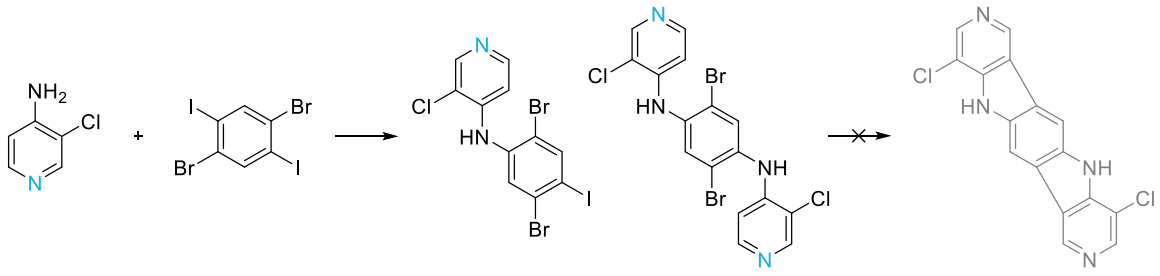

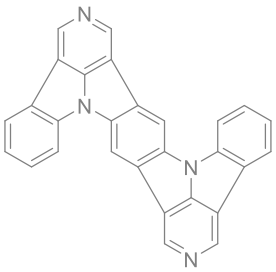

A.1.3 The Carboline Approach

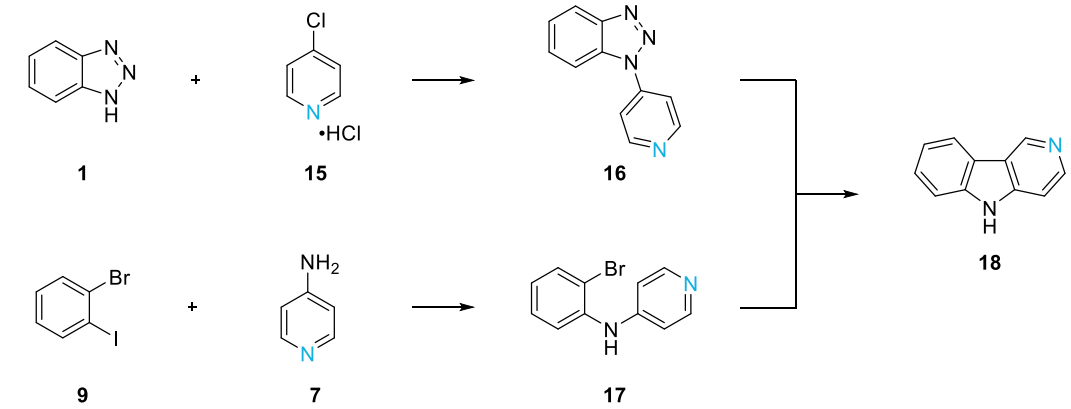

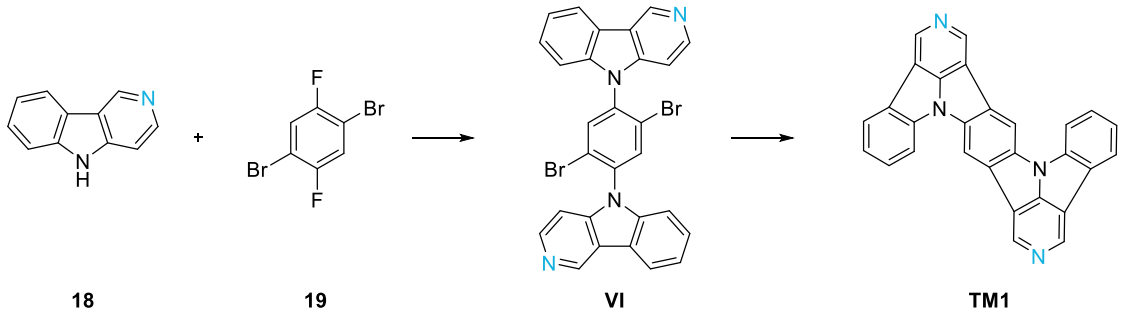

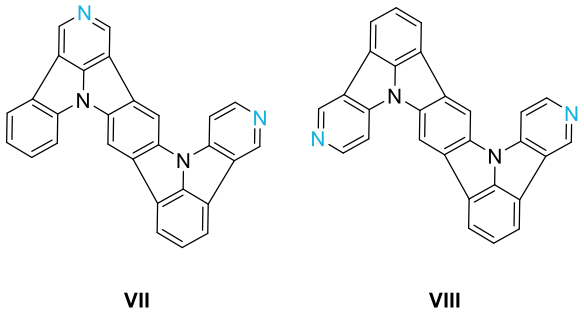

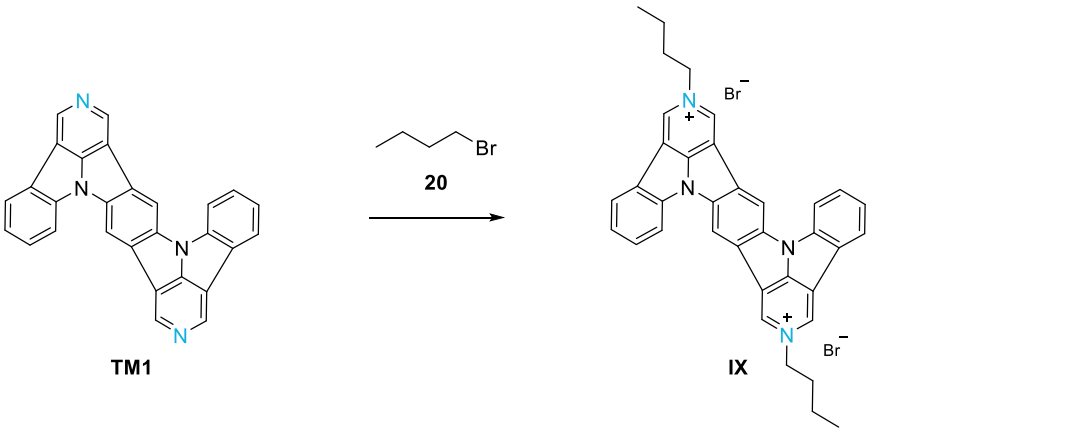

A.1.4 The Diazotization Approach

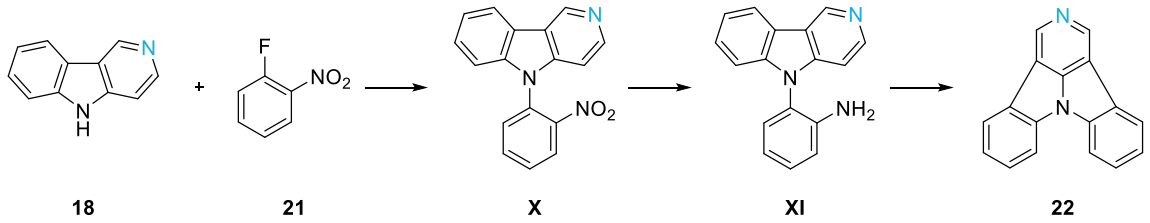

18 21 X XI 22

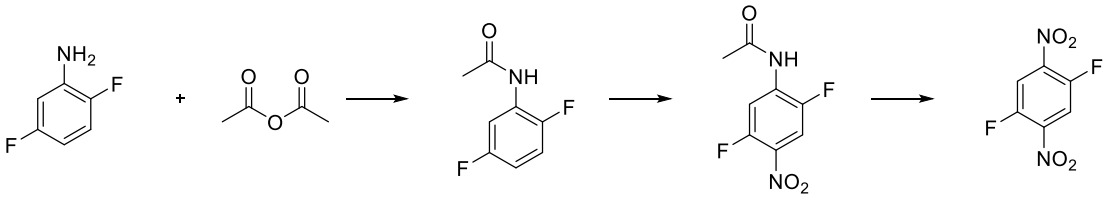

23 24 25 26 27

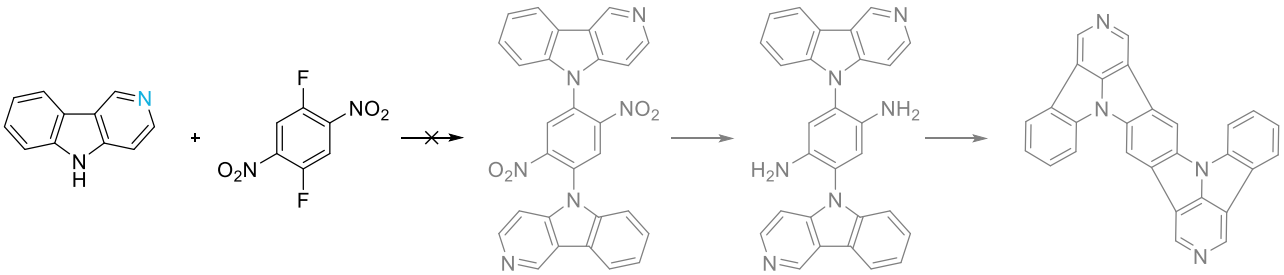

18 27 XII XIII TM1

A.2 Target Molecules TM2

A.2.1 Alkyne-linked 5NICz

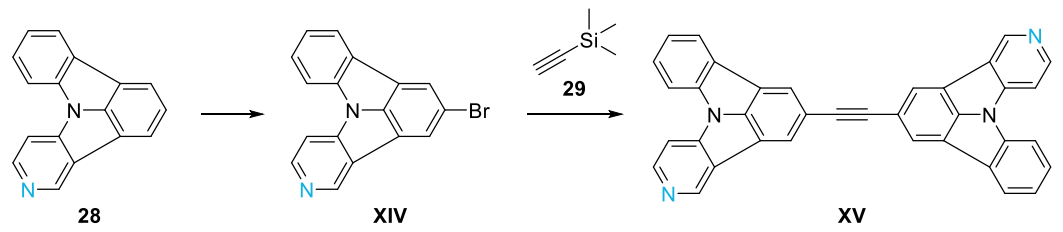

A.2.2 5,11NICz Building Block

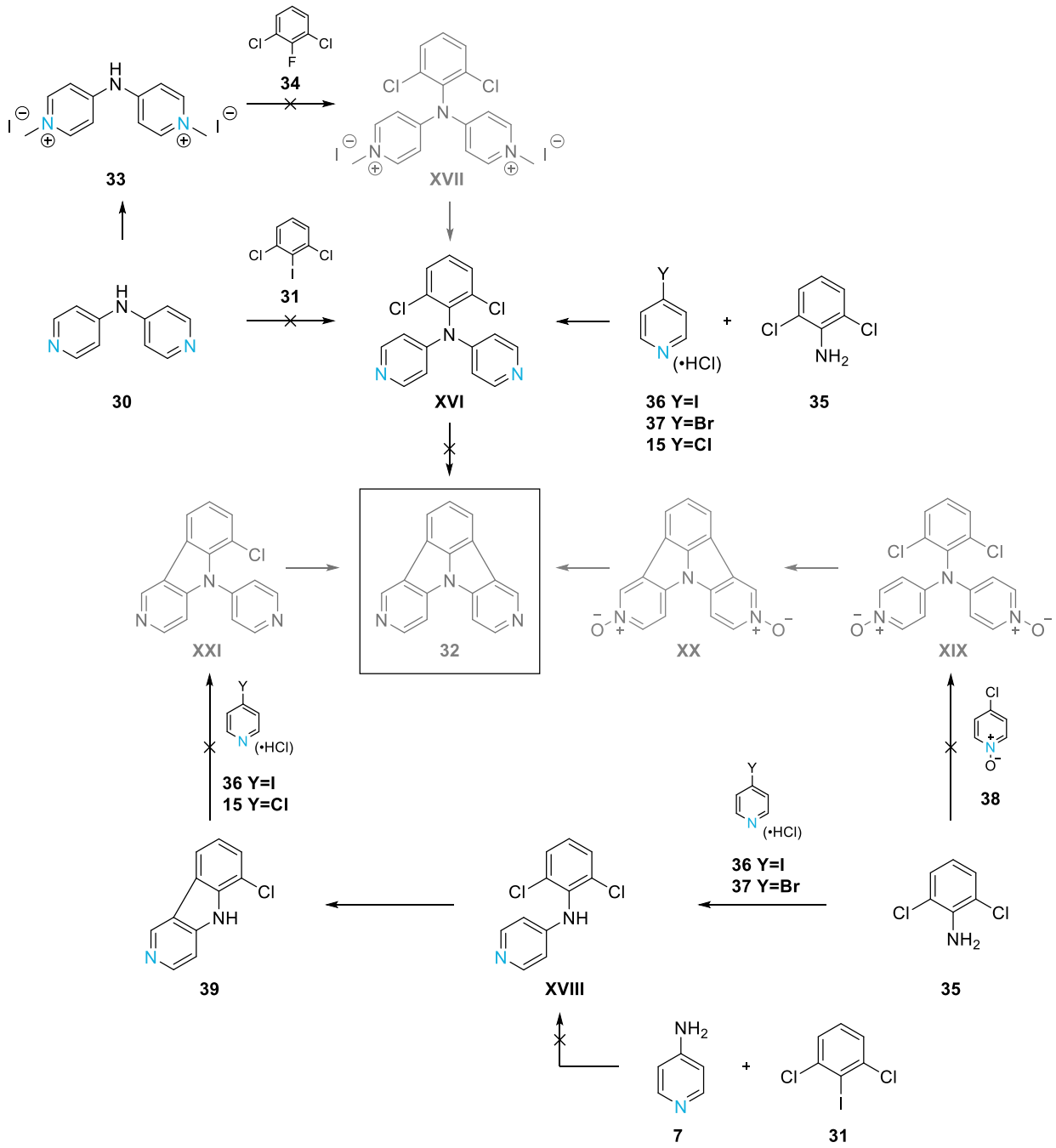

A.3 7,9NICz Building Block for Target Molecule TM3

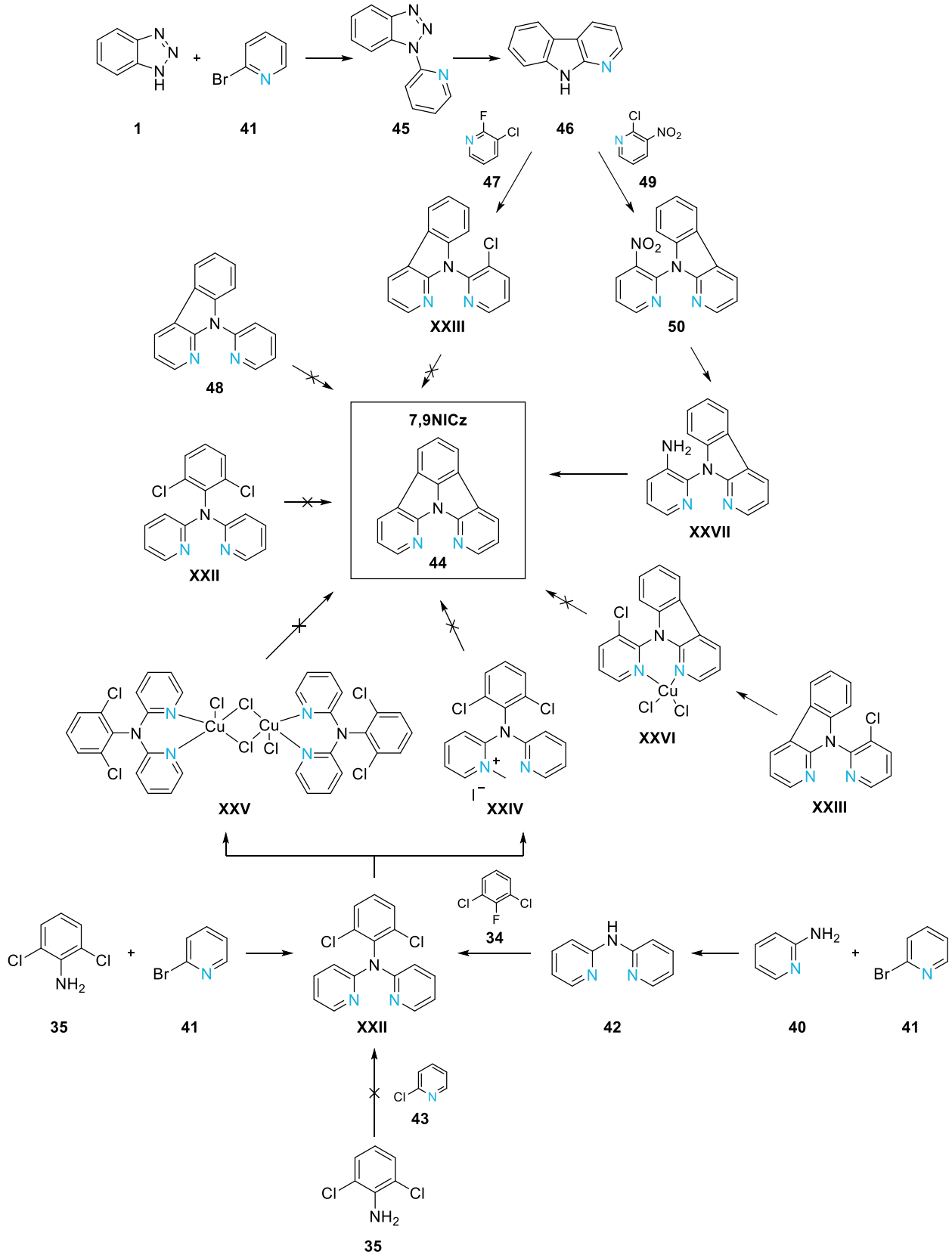

A.4 Catalysts

A.4.1 (NHC)Pd(allyl)Cl

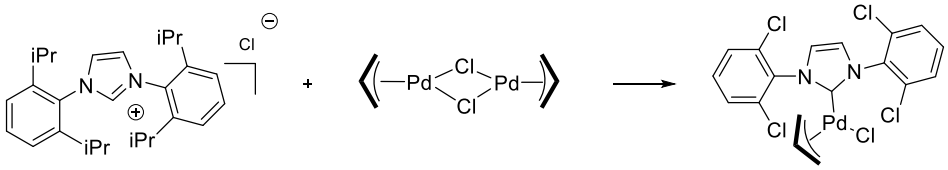

51 52 53

A.4.2 Cu(Xantphos)I

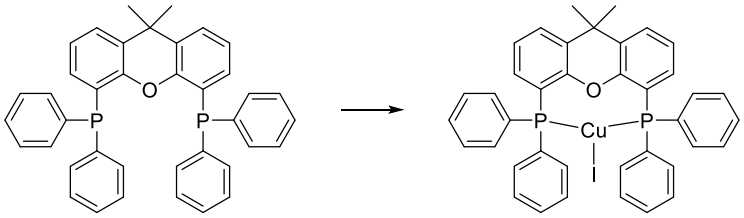

54 55

B. General Part

B.1 Organic Electronics

In the last decades intensive research efforts focused on the field of organic electronics. Due to the facile deposition of organic films on low-cost substrates such as glass, plastics or foils, devices based on organic materials are of increased importance in commercial applications. Such functional organic materials are used in organic light emitting diodes (OLEDs), organic field-effect transistors (OFETs) or organic photovoltaics (OPVs), to name just a few.[1], [2], [3]

These organic materials known as organic semiconductors are based on π-conjugated polymers or small molecules. For the latter category, in particular polycyclic aromatic and heteroaromatic molecules like substituted anthracene derivatives and arylamine containing materials are of great importance.[4], [5]

B.2 OLEDs

Organic light emitting diodes (OLEDs) are already used in applications for display technologies like smartphones and large area TV screens, but also the use in lighting becomes increasingly more appealing.

The working principle is based on electroluminescence, where an organic semiconductor is placed between an anode and a cathode and voltage is applied. At the anode holes are injected into the HOMO and at the cathode electrons are injected into the LUMO of the organic material. The electrons and holes recombine to form excited electron-hole pairs, so-called excitons, which emit light upon relaxation.[3] A graphic depiction of the working principle adapted from Shirota and Kageyama[3] is shown in Figure 1.

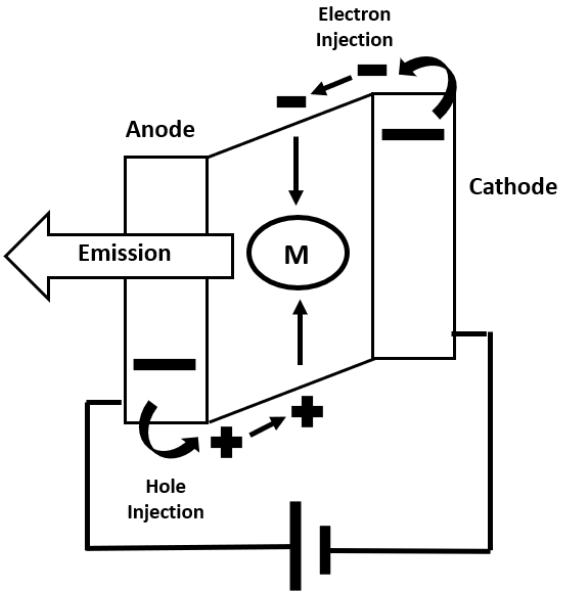

Figure 1: Working principle of OLEDs

The simplest structure of an OLED is a single emissive layer sandwiched between the two electrodes, which leads to poor efficiency and brightness. More efficient light emission, good electron- and hole-injection as well as transport properties in an OLED device requires a multilayered structure, where two or more materials with different charge transport characteristics are used. Hole- and electron-transporting layers between the electrodes and the emissive layer allow a more balanced charge carrier transport.[6]

B.3 Types of OLEDs

Fluorescence based emitters, which were used in first generation OLEDs, can only utilize singlet excitons. However, in electroluminescent devices the ratio of singlet and triplet excitons is 1:3 and therefore fluorescent OLEDs can only reach a theoretical maximum of 25% internal quantum efficiency. The development of phosphorescent emitters for OLED devices (PhOLEDs) by Baldo et al.[7] lead to an increase to 100% theoretical internal quantum yield, since those emitters can use both singlet and triplet excitons simultaneously through intersystem crossing (ISC). A major drawback of PhOLEDs is the use of heavy transition metals, as they rise concerns regarding toxicity, rarity and high fabrication costs.[8]

To overcome the limitations and concerns of fluorescence and phosphorescence based OLED devices, the first fully organic emitter for high efficiency OLEDs, reported by Endo et al.,[9] utilized the mechanism of thermally activated delayed fluorescence (TADF). TADF emitters are able to use both singlet and triplet excitons and therefore can theoretically reach an internal quantum yield of 100%. When the singlet-triplet energy-gap is sufficiently small, the triplet excited state can be up-converted to the singlet state by reversed intersystem crossing (RISC). Therefore, TADF-OLEDs produce photoluminescence from prompt fluorescence of the singlet excited state and delayed fluorescence, which is a result of RISC from triplet into singlet up-conversion.[10], [11]

B.3.1 Host Materials

High concentration of triplet excitons is a problem in any OLED device harvesting light from triplet excited states due to relatively long lifetime. This results in triplet-triplet annihilation and subsequently efficiency roll-off.[8], [12], [13]

To prevent these quenching effects, the emitters (the guests) need to be dispersed in an organic matrix, a so-called host material. The host materials also play a significant role in device performance and therefore must fulfill certain requirements. To avoid an energy transfer from the guest back to the host, it is crucial that the triplet energy of the host material is higher than that of the emitter. Also, suitable HOMO and LUMO levels of the host, matching those of the emitter and the adjacent layers, are required to facilitate charge injection and subsequently lower the device driving voltages. Thermal stability is also an important factor, since it influences performance and lifetime of the

device. At last, host materials should have balanced charge transport properties, which is realized by bipolar molecules.[14], [15], [16]

B.3.2 Bipolar Host Materials

Bipolar host materials contain both donor and acceptor subunits within one molecule. However, combining donor and acceptor in a single molecule usually leads to lower triplet energies due to intramolecular charge transfer. To decrease the donor-acceptor interactions in bipolar host materials and thus maintain the high triplet energies, it is important to reduce the conjugation within the system. Our research group recently introduced novel bipolar host materials with electron-accepting oxadiazole scaffold and electron-donating triarylamine subunits.[14]

With increased planarization from triphenylamine (TPA) to phenylcarbazole (PCz) and indolo[3,2,1-*jk*]carbazole (ICz), which is shown in Figure 2, the donor strength decreases. This is due to the contribution of the nitrogen lone pair to the aromaticity of the pyrrole subunit. As a result, the intramolecular charge transfer is reduced, and higher triplet energies are achieved. [17]

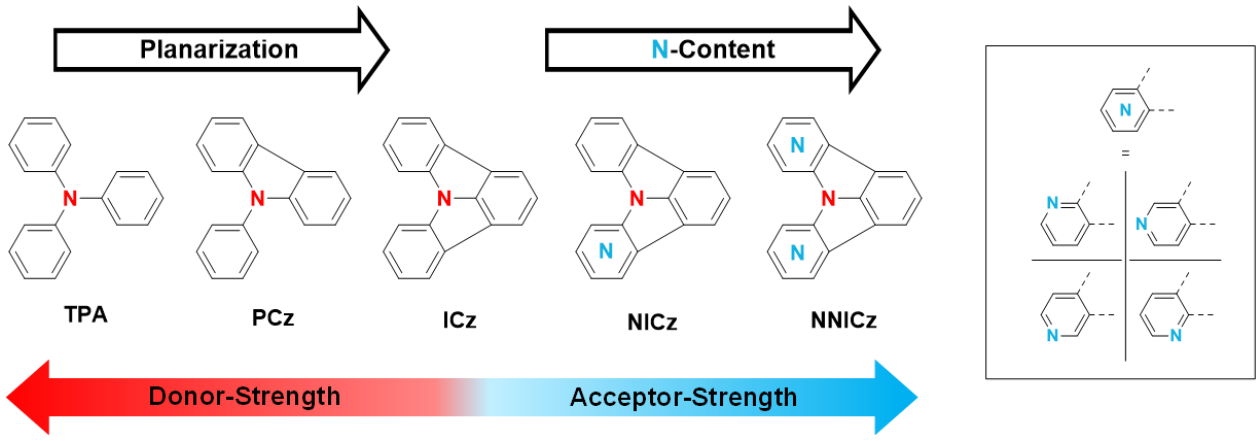

Figure 2: Concept of modifying donor and acceptor strength by planarization of triphenylamine and incorporation of pyridine nitrogen[17]

B.4 Nitrogen Incorporated Indolo[3,2,1-*jk*]carbazole (NICz)

It was shown, that besides the donor properties, ICz also exhibits weak acceptor properties. To further increase the acceptor strength, electron-withdrawing pyridine-like nitrogen atoms were incorporated into the ICz scaffold (NICz) with different positioning and amount of nitrogen, also shown in Figure 2. The impact of the nitrogen atoms in the NICz building blocks were investigated in our research group.

Changing the nitrogen position affects electrochemical properties, such as HOMO and LUMO energy levels and absorption as well as emission maxima of the NICz building blocks.

Figure 3 shows the different HOMO and LUMO energy levels as well as absorption and fluorescence spectra of two selected NICz examples in comparison to ICz. This example elucidates the different impact of nitrogen incorporation in para (5NICz) and meta (6NICz) position to the central nitrogen atom.

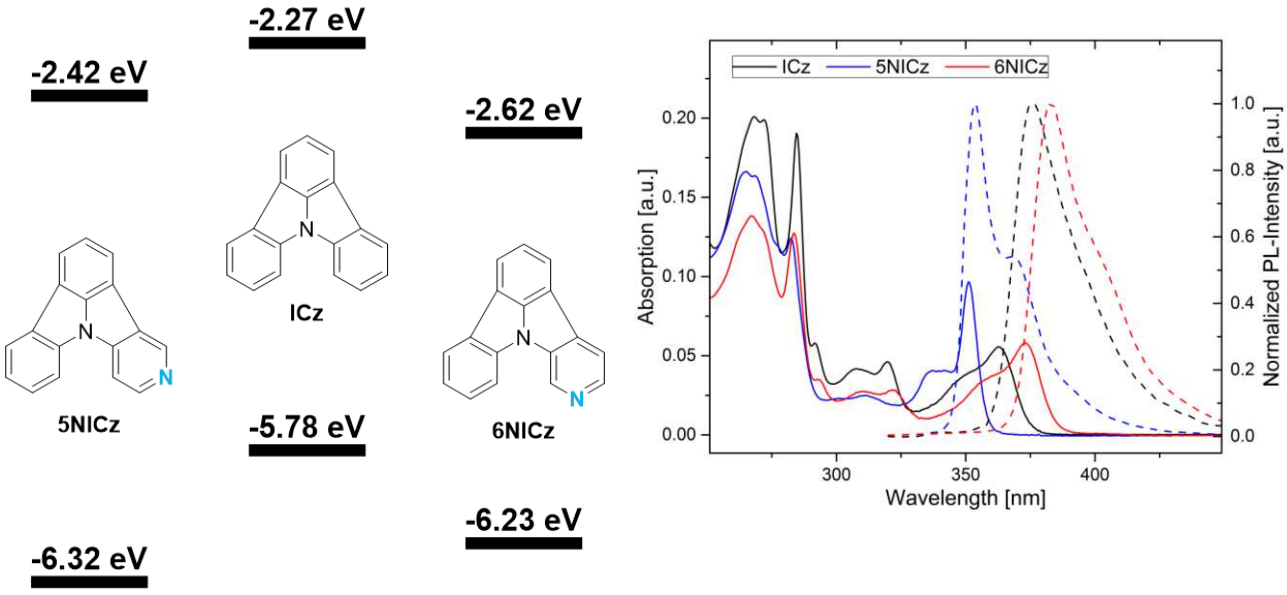

Figure 3: Influence of nitrogen position in NICz on HOMO/LUMO energy levels (left) and absorption and emission maxima (right)[17]

In general, by incorporation of pyridine-like nitrogen into the ICz scaffold, the energy of both orbitals (highest occupied and lowest unoccupied molecular orbital) decreases compared to ICz. Clear trends for the extent of the decrease in dependence on the nitrogen position were observed. As for fluorescence characteristics, 5NICz with an emission maximum of 354 nm blueshifted compared to the ICz scaffold (emission maxima 375 nm), whereas 6NICz is redshifted with an emission maximum of 384 nm.[17]

Different positioning of the nitrogen also leads to different orientation and packing in the crystallin state due to non-classical C-H···N hydrogen bonds.[17] This is shown on the 5NICz and 2NICz

building block, where in both cases the pyridine nitrogen is in para position to the central nitrogen atom (Figure 4).

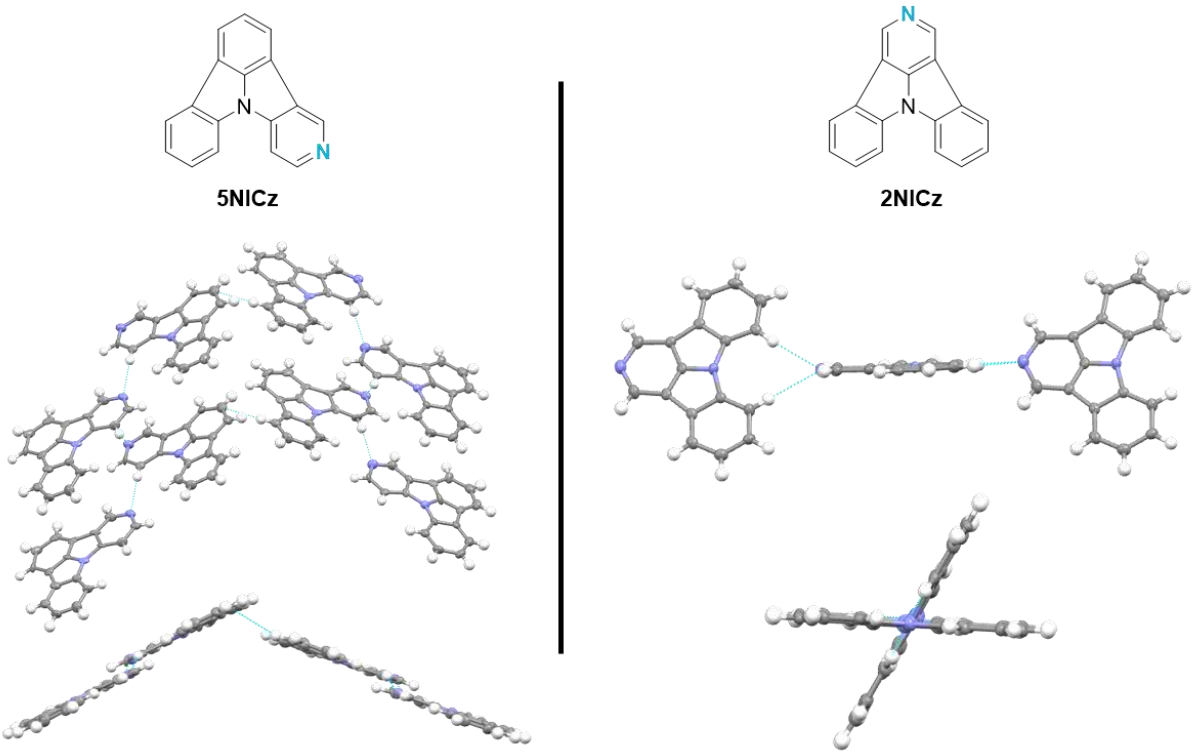

Figure 4: Influence of nitrogen position on crystal packing, 5NICz (left) and 2NICz (right)[17]

Due to the hydrogen bonding, the 2NICz molecules form straight chains with every other molecule twisted in a 63.4° angle. The chains connect to layers by π-stacking interactions, are parallel and extend in opposite directions. The 5NICz molecules also form chains in the solid state with every other molecule rotated 90° in the plane. The chains connect by π-π interactions in a zig-zag style.[17]

This knowledge of HOMO and LUMO energy levels, which are an important factor for charge transport and injection in electronic devices, as well as the impact on the crystal packing, which has significant influence on photophysical and electronic properties of thin films in organic materials,[18] allows to design new functional materials based on the NICz scaffold with tailored properties.

B.5 Aim of the Thesis

The aim of this thesis was to incorporate the NICz scaffold into larger systems and induce different electrochemical and photophysical properties by changing the position of the nitrogen atoms. Considering the recent research in our group, which is described in chapter B.4, different orientation and packing in the crystalline state due to non-classical C-H···N hydrogen bonds should be investigated in these NICz based systems. A schematic representation of target molecules is shown in Scheme 1, a more detailed description of the different targets will be given at the beginning of the next chapter.

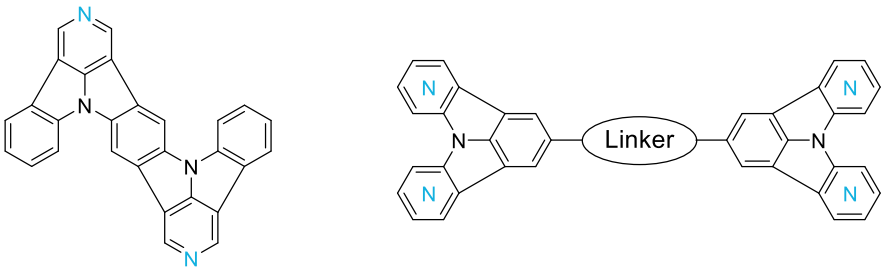

Scheme 1: Schematic representation of target molecules

C. Specific Part

C.1 Introduction

The main focus of this work was to incorporate the NICz structure motif into larger systems and control their solid state alignment. The previously gained insights on the effect of different nitrogen positions on the crystallization behavior of several NICz systems should be used to induce specific arrangement and packing within the solid state of the novel materials.

As described in chapter B.4, the 2NICz building block with the nitrogen atom in para position forms linear chains, but with every other molecule twisted in a certain angle (see Figure 4, right). This alignment should be used in a larger, fully planar NICz based system, but by incorporating a second nitrogen atom the distortion should be prevented. With nitrogen atoms on both sides in para position, target molecule **TM1**, which is shown in Scheme 2, is expected to form fully planar lines due to the C-H···N hydrogen bonds and additionally can stack on each other by π-π interactions. This intense, highly ordered stacking is expected to promote conductivity, therefore making **TM1** a promising candidate for application in OLEDs or OFETs.

TM1

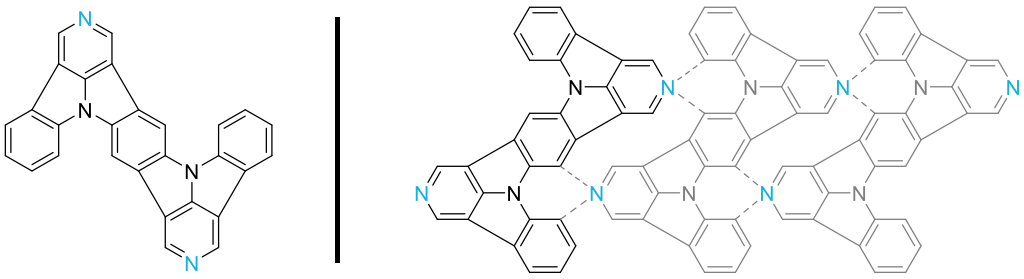

*Scheme 2: Target molecule **TM1***

Furthermore, materials based on the target scaffold **TM2** (Scheme 3, left) with literature known NICz building blocks with different positions and amount of nitrogen and various linkers should be synthesized for investigation of their crystallization behavior.

In this work the **alkyne-linked 5NICz** was synthesized starting from 5NICz, which is shown in Scheme 3 on the top right side.

The building block **5,11NICz**, which is shown in Scheme 3 on the bottom right, is also known to the literature, but in the synthesis reported from Kader et al.[17] **5,11NICz** only forms as minor isomer with low yields. Therefore, part of this work was to find an alternative synthetic route for the selective preparation of **5,11NICz**, suitable also for large scale preparation, for the use as a building block in the synthesis of molecules like **TM2**.

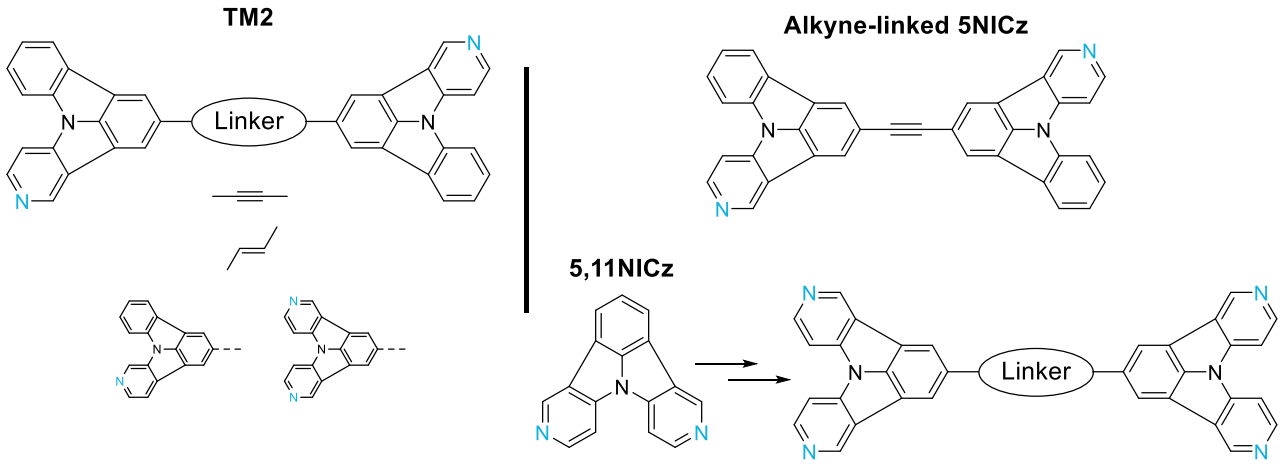

*Scheme 3: Concept of target molecules **TM2** (left), **Alkyne-linked 5NICz** and **5,11NICz** building block (right)*

Furthermore, a NICz building block (**7,9NICz**) for target molecule **TM3** should be synthesized. The nitrogen substitution pattern of this molecule is of special interest because of its expected coordination properties. **TM3** is aimed to be used for self-organized, multidimensional networks either through classical N-H···N hydrogen bonds or through metal ion coordination (Scheme 4).

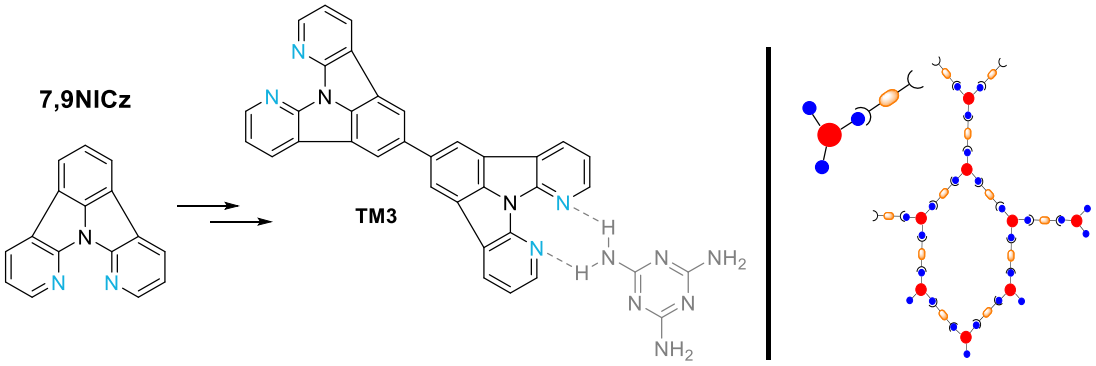

*Scheme 4: Building block for target molecule **TM3***

C.2 Synthesis of Target Molecule TM1

Four different retrosynthetic approaches were considered to synthesize target molecule **TM1**. Two approaches are designed with functional groups on the pyridine unit to form the desired product in a ring closing C-H activation (CHA). The other two approaches form the product either through CHA or diazotization reaction, but due to the position of the functional groups more different structural isomers are likely to form in the ring closing step.

C.2.1 The Bromo-carboline Approach

Since target molecule **TM1** is a symmetrical molecule, the first retrosynthetic approach, which is shown in Scheme 5, is a nucleophilic substitution reaction (S_N) or C-N coupling reaction of halogenated γ-carboline and a benzene derivative followed by a two-sided CHA as the ring closing step. In this approach the halogen (X) is located at the carboline rather than the benzene unit to reduce the amount of possible isomers formed (for comparison see C.2.3).

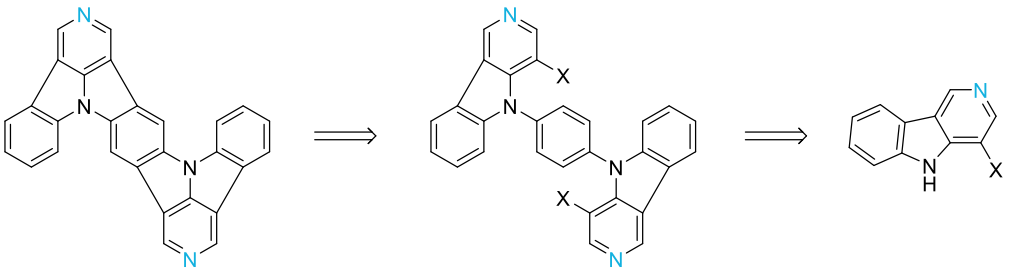

*Scheme 5: The bromo-carboline approach towards **TM1***

For the synthesis of brominated γ-carboline (**4**) (Scheme 6) first a nucleophilic substitution reaction of benzotriazole (**1**) and 3-bromo-4-chloropyridine (**2**) in toluene using a literature procedure from Xu et al.[19] followed by a modified Graebe-Ullmann reaction in polyphosphoric acid according to Robinson and Thornley[20] were performed. Careful temperature control is important in the Graebe-Ullmann reaction, because the strongly exothermic reaction tends to runaway while foaming when heated too fast. Keeping in mind that the starting materials are of low cost and the synthesis can be performed in large scale without any catalyst, the used method is convenient for the preparation of **4**, despite the low yields in the product forming step.

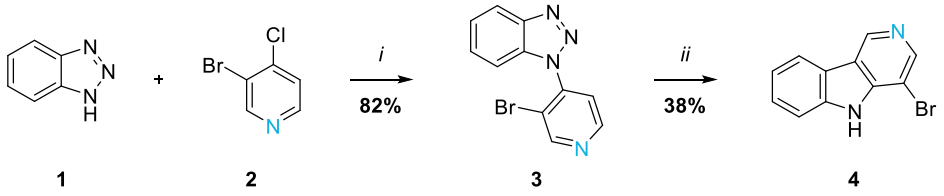

*Scheme 6: Synthesis of **4***

*i) S_N reaction of **1** and **2**, toluene, reflux; ii) Graebe-Ullmann reaction of **3**, polyphosphoric acid, 140 °C*

Different conditions for nucleophilic substitution reaction with 1,4-difluorobenzene (**5**) and Buchwald-Hartwig amination (BHA) or Ullmann condensation with 1,4-diiodobenzene (**6**) were investigated for the formation of compound **I**. Neither the nucleophilic substitution reactions nor the coupling reaction yielded the desired product. There was no conversion or decomposition of the starting materials detected. The reactions are shown in Scheme 7 and the different reaction conditions, which were tested, are summarized in Table 1.

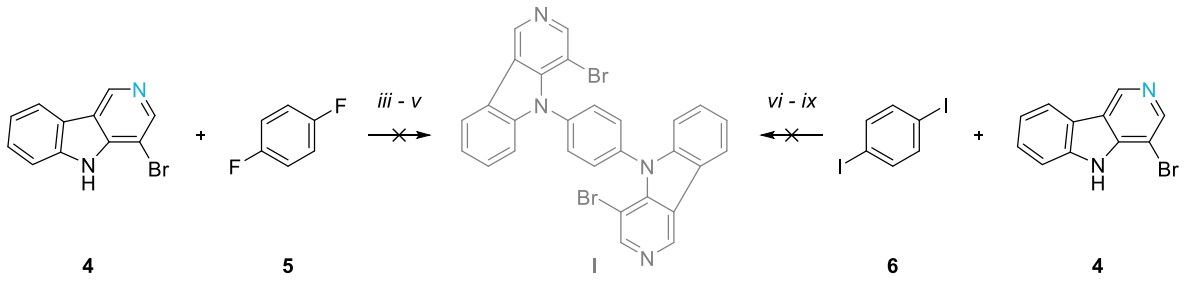

*Scheme 7: Synthesis towards **I***

*iii – v) S_N reaction of **4** and **5;** vi – ix) Coupling reactions of **4** and **6***

*Table 1: Conditions for synthesis towards compound **I***

	Reaction type	Catalyst, Ligand	Base	Solvent	T [°C]
iii	S_N	-	Cs_2CO_3 (1.2 eq)	DMF	130
iv	S_N	-	Cs_2CO_3 (1.1 eq)	DMSO	120
v	S_N	-	NaH (4.2 eq)	DMF	40-110
vi	Ullmann	Cu (0.06 eq) 18-Crown-6 (0.12 eq)	NaO^tBu (3 eq)	Toluene	110
vii	Ullmann	Cu (1 eq)	K_2CO_3 (1.5 eq)	DMF	130
viii	BHA	$Pd_2(dba)_3$, ($^tBu_3PH)BF_4$ (0.08 eq)	NaO^tBu (6 eq)	Toluene	110
ix	BHA	$Pd(dba)_2$, rac-BINAP (0.08 eq)	NaO^tBu (6 eq)	Toluene	110

C.2.2 The Di(chloro-carboline) Approach

Since the first strategy failed, the second synthetic approach shown in Scheme 8 was developed to synthesize target molecule **TM1** with X and Y being different halogen atoms. With this approach any issues regarding selectivity of the final CHA step can be avoided.

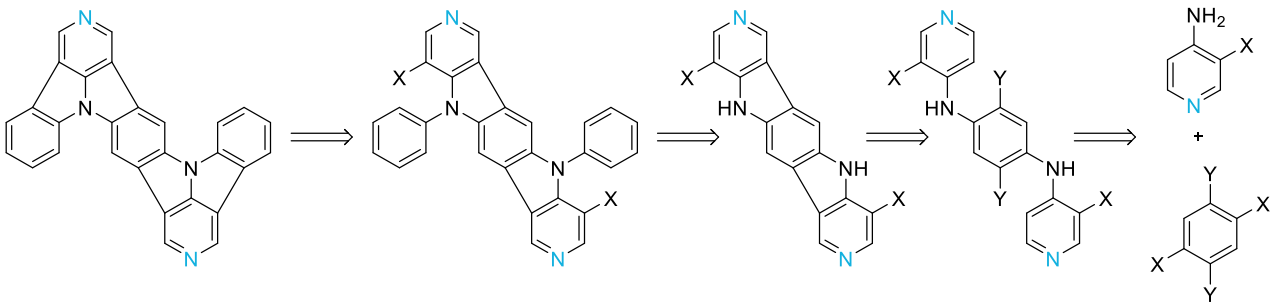

*Scheme 8: The di(chloro-carboline) approach towards **TM1***

The feasibility of the initial CHA of the intermediate containing multiple halogens towards the annulated carboline derivative was first tested using the smaller model system **11**, which is shown in Scheme 9.

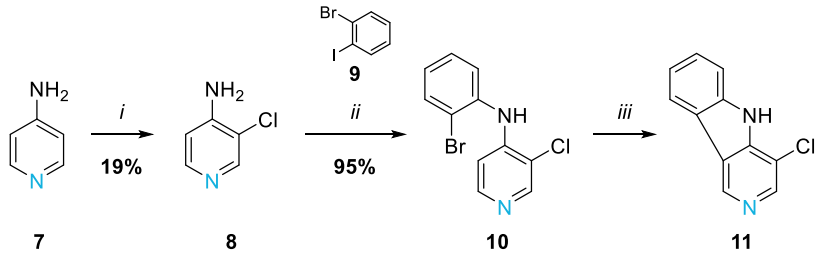

*Scheme 9: Synthesis of smaller model system **11***
*i) Chlorination of **7**, NCS, ACN, rt; ii) BHA of **8** and **9**, $Pd_2(dba)_3$, dppf, NaO^tBu, toluene, 110 °C;*
*iii) CHA of **10**, (NHC)Pd(allyl)Cl, K_2CO_3, DMA, 130 °C*

The test system **11** was synthesized by starting with the chlorination of 4-aminopyridine (**7**) with NCS *via* electrophilic aromatic substitution. NCS was added in small portions until no starting material **7** was left, unfortunately this led to the formation of significant amounts of byproduct with chlorine substitution in positions 3 and 5, therefore resulting in low yield of the desired product. The next step is a BHA with 4-amino-3-chloropyridine (**8**) and 1-bromo-2-iodobenzene (**9**), which gave **10** in almost quantitative yield. For ring closing a CHA protocol previously introduced in our research group[14] was performed to give a 1:1 mixture of starting material **10** and product **11**. Since this was only a model system towards **TM1**, the crude product was not purified.

The catalyst (NHC)Pd(allyl)Cl (**53**) for the CHA was synthesized according to the procedure of Navarro and Nolan,[21] which is shown in Scheme 10.

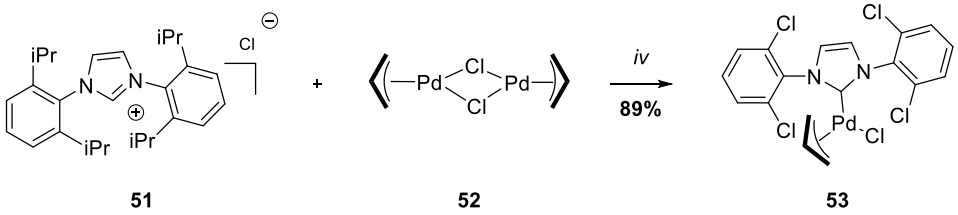

51 52 53

*Scheme 10: Synthesis of NHC-based catalyst **53***
*iv) **51** and **52**, n-BuLi, THF, rt*

Since this procedure worked for the test system **11**, it was applied for the synthesis towards target molecule **TM1** (Scheme 11).

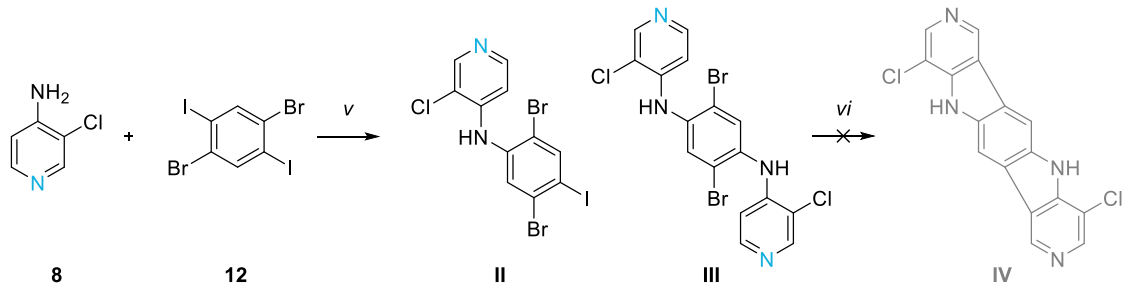

8 12 II III IV

*Scheme 11: Synthesis towards **IV***
*v) BHA of **8** and **12**, Pd(dba)$_2$, rac-BINAP, NaO^{t}Bu, toluene, 110 °C; vi) CHA of **II** and **III**, (NHC)Pd(allyl)Cl (**53**), K_2CO_3, DMA, 130 °C*

Starting with the BHA with 4-amino-3-chloropyridine (**8**) and 1,4-dibromo-2,5-diiodobenzene (**12**), initially only intermediate **II** was observed during the reaction and only after about one week and daily addition of more catalyst and ligand small quantities of the desired product **III** were formed.
On a small-scale synthesis (0.8 mmol) separation of **II** and **III** could be achieved by column chromatography to yield 14% of the desired product **III**. However, performing the synthesis on a larger scale (4.6 mmol), separation attempts using liquid chromatography and crystallization failed. Therefore, the ring closing CHA was performed with the mixture with no formation of the product, neither the one-sided nor the two-sided product **IV**.
Since in the BHA step (*v*) some product (**III**) formation was observed upon addition of more catalyst, it was assumed that the iodine from the precursor deactivated the catalyst. Therefore, another benzene precursor without iodine was used for the synthesis of **IV**, which is shown in Scheme 12.

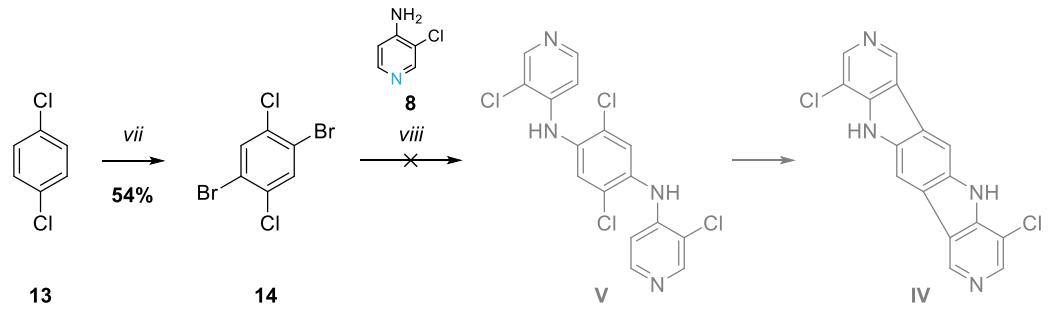

*Scheme 12: Alternative synthesis towards **IV***

*vii) Bromination of **13**, Br_2, Fe, $CHCl_3$, reflux; viii) BHA of **14** and **8**, $Pd(dba)_2$, rac-BINAP, NaO^tBu, toluene, 110 °C*

The bromination of 1,4-dichlorobenzene (**13**) was performed according to W. H. Lai et al.[22] with bromine and iron in chloroform with acceptable yields. The next step was the same BHA protocol as described above, however only the one-sided intermediate and no product **V** was formed.

C.2.3 The Carboline Approach

Since the first two strategies to selectively form target molecule **TM1** did not work, nucleophilic substitution reaction of γ-carboline with halogenated benzene (X and Y being different halogen atoms) and two-sided CHA for ring closing was performed (Scheme 13). The major disadvantage of this approach is the possible formation of the three different isomers during the final ring closing step.

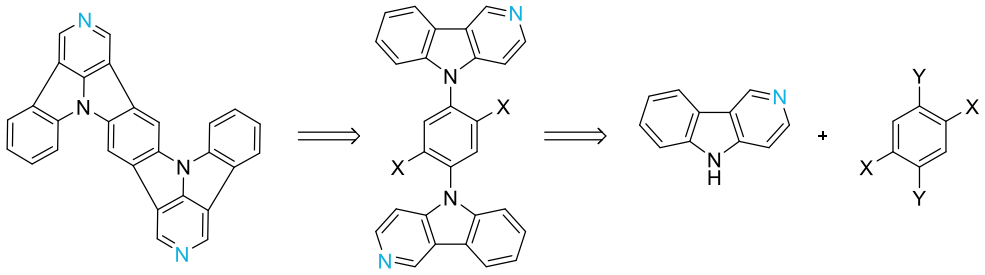

*Scheme 13: The carboline approach towards **TM1***

The γ-carboline (**18**) can be synthesized *via* two different routes, which are shown in Scheme 14.

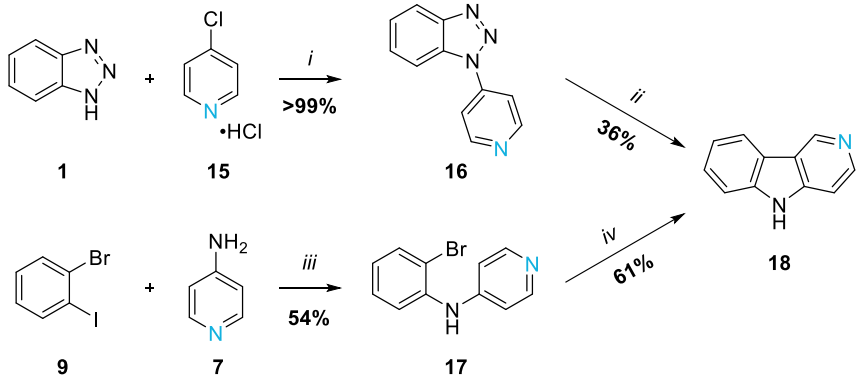

*Scheme 14: S_N reaction and Graebe-Ullmann route (top row), metal-assisted route (bottom row) to **18***
*i) S_N reaction of **1** and **15**, toluene, reflux; ii) Graebe-Ullmann of **16**, polyphosphoric acid, 140 °C;*
*iii) BHA of **9** and **7**, $Pd_2(dba)_3$, dppf, NaO^{t}Bu, toluene, 110 °C: iv) CHA of **17**, $Pd(OAc)_2$, Na_2CO_3, DMF, 160 °C*

The first route, which is shown in Scheme 14 top row, is a nucleophilic substitution reaction of benzotriazole (**1**) and 4-chloropyridine hydrochloride (**15**) in toluene following the procedure of Xu et al.,[19] which gave **16** in quantitative yield, followed by a modified Graebe-Ullmann reaction in polyphosphoric acid according to Robinson and Thornley.[20] The second route (Scheme 14 bottom row) is metal assisted starting with a BHA using 1-bromo-2-iodobenzene (**9**) and 4-aminopyridine (**7**), followed by a CHA for ring closing to give **18** in moderate yield. Both synthetic routes are short, easy to handle and work quite fine. However, the metal assisted route needs relatively expansive catalysts in both steps compared to the starting materials of the first route. Therefore, the synthetic route starting from the benzotriazole (**1**) was preferable used for a large-scale synthesis of **18**.

The synthesis of target molecule **TM1** is shown in Scheme 15.

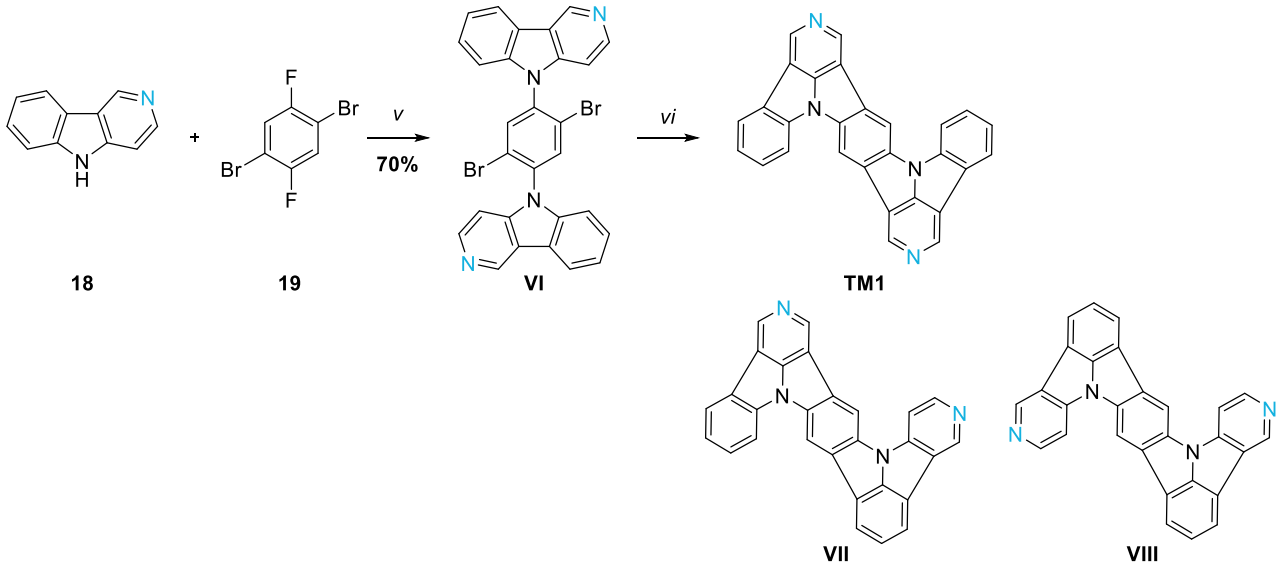

*Scheme 15: Synthesis of **TM1***
*v) S_N of **18** and **19**, Cs_2CO_3, DMF, 130 °C; vi) CHA of **VI**, (NHC)Pd(allyl)Cl, K_2CO_3, DMA, 130 °C*

The first step was a nucleophilic substitution reaction of γ-carboline (**18**) and 1,4-dibromo-2,5-difluorobenzene (**19**). Two different compounds with the same mass (LC-MS), but different R_f values were separated *via* liquid chromatography. For NMR characterization, one compound was only soluble in $CDCl_3$ and the other one in DMSO-*d*6. However, MS and NMR experiments indicate, that those two components are the same desired product **VI**, but could be rotamers to each other. The ring closing CHA was performed with both compounds separately as well as a mixture with no significant difference in reaction behavior or yield. Therefore, ring closing CHA to target molecule **TM1** on larger scale was performed using a mixture. As already mentioned above, since the bromines are on the benzene unit of compound **VI**, three different isomers can form due to the rotation of the single bond between the benzene and the carboline units. The three isomers **TM1**, **VII** and **VIII** form in a ratio of about 3:1:1 (calculated by NMR) and could not be separated *via* crystallization or sublimation, because these isomers only differ in the position of the nitrogen and show very similar properties. Also, separation *via* liquid chromatography could not be performed due to limited solubility.

To improve the solubility of the crude mixture and facilitate separation *via* liquid chromatography, butyl chains were attached at the pyridine nitrogen to form a pyridinium salt. The synthesis was performed following the procedure of Porter, Vaid and Rheingold.[23] The mixture of **TM1**, **VII** and **VIII** with 1-bromobutane (**20**) was heated to reflux in DMA, which is shown in Scheme 16.

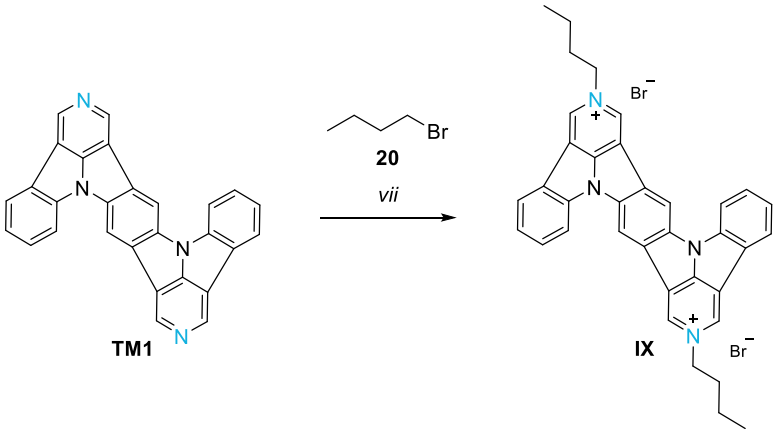

*Scheme 16: Alkylation strategy for the isomers **TM1**, **VII** and **VIII**, based on the example of **TM1***
*vii) Alkylation of **TM1**, 1-bromobutane **20**, DMA, 150 °C*

Analytical tests using reversed phase HPLC with ACN and methanol as liquid phase showed a separation of three products, but unfortunately the solubility of the butylated pyridinium salt was too low for performing preparative HPLC.

C.2.4 The Diazotization Approach

In an additional approach depicted in Scheme 17 ring closing towards **TM1** is achieved *via* diazotization reaction. This methodology was already successfully employed for the first reported synthesis of ICz.[24]

The first step would be a nucleophilic substitution reaction, then a reduction of the nitro groups to the amino compound and the final ring closing step *via* diazotization.

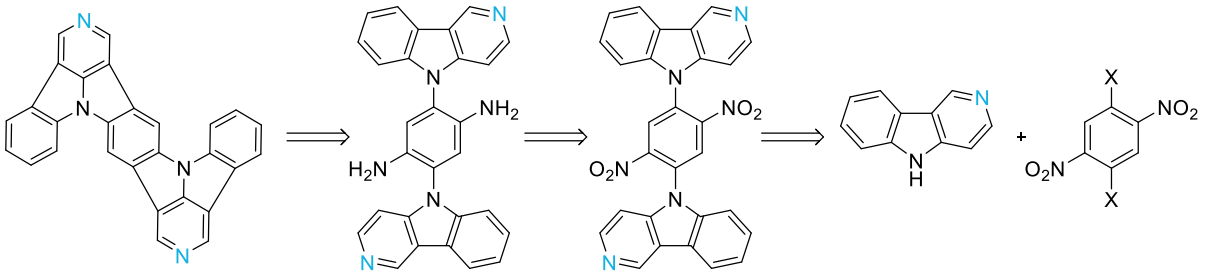

*Scheme 17: The diazotization approach to **TM1***

To investigate the selectivity of the diazotization step, this approach was first tested with the corresponding 2NICz **22**. The synthesis is shown in Scheme 18.

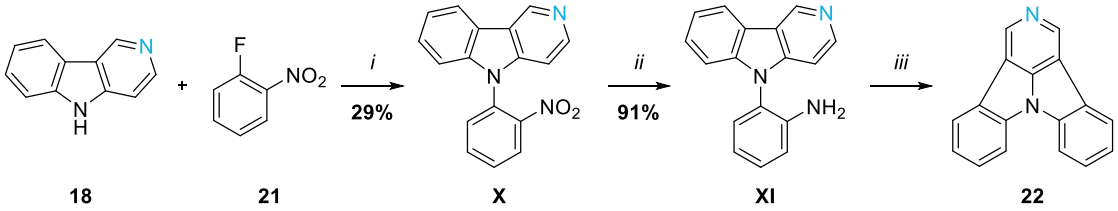

*Scheme 18: Synthesis of smaller model system **22***

*i) S_N reaction of **18** and **21**, Cs_2CO_3, DMF, 130 °C; ii) Reduction of **X**, $SnCl_2{\cdot}2H_2O$, EtOH, reflux;*

*iii) Diazotization of **XI**, $NaNO_2$, AcOH, H_2SO_4, H_2O*

γ-Carboline (**18**) and 1-fluoro-2-nitrobenzene (**21**) were reacted in a nucleophilic aromatic substitution to the nitro compound **X** with Cs_2CO_3 serving as a base. The next step was a reduction of the nitro group to the amino group using $SnCl_2{\cdot}2H_2O$ to yield **XI**. Ring closing was performed *via* diazotization reaction to form the product **22**. GC-MS only showed one peak with the product mass. However, the crude NMR spectrum indicated, that different molecules have been formed. TLC with a reference material confirmed the presence of the desired product within the reaction mixture. Since this was only a model system for target molecule **TM1** and the synthesis was only performed on a small scale, product **22** was not purified and therefore no yield was determined.

The precursor 1,4-difluoro-2,5-dinitrobenzene (**27**) for the synthesis of target molecule **TM1** was synthesized following the procedure of Fagan et al.[25] in a three-step synthesis without any purification in between. The synthesis is shown in Scheme 19.

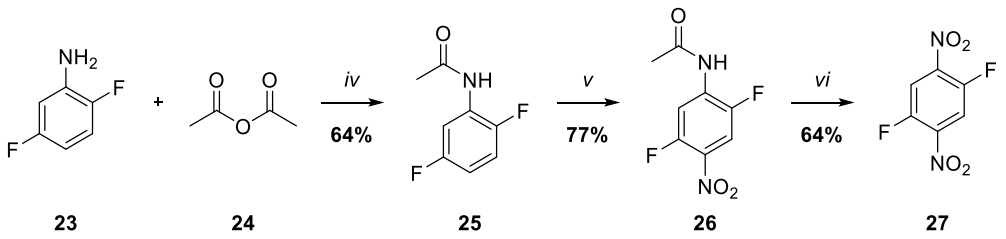

*Scheme 19: Synthesis of **27***
*iv) Acetylation of **23** with **24**, MeOH, rt; v) Nitration of **25**, H_2SO_4, HNO_3, 0 °C;*
*vi) One-pot deprotection and oxidation of **26**, H_2O_2, $MeSO_3H$, 55 °C*

The amino group of commercially available 2,5-difluoroaniline (**23**) was protected by acetylation with acetic anhydride to form **25**. Nitration in para position to the protected amino group gave **26**, followed by a one-pot deprotection and oxidation of the amino group to form 1,4-difluoro-2,5-dinitrobenzene (**27**) with 32% overall yield.

Unfortunately, no reaction of **18** and **27** occurred using the same conditions that were used for the small model system **22**. The synthesis towards **XII** is shown in Scheme 20.

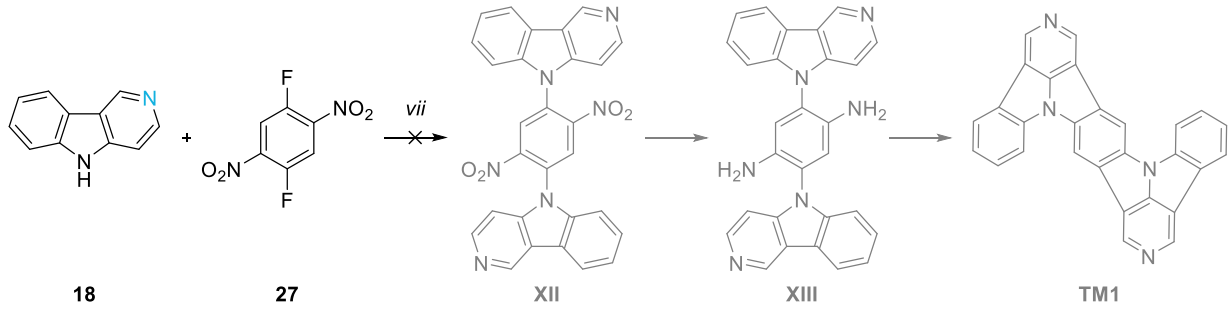

*Scheme 20: Synthesis towards **XII***
*vii) S_N reaction of **18** and **27**, Cs_2CO_3, DMF, 130 °C*

C.3 Target Molecules TM2

Already literature known NICz building blocks with different position and amount of nitrogen should be used to synthesize target molecule **TM2** using alkyne or alkene linkers to investigate the influence of the nitrogen atoms in those systems on electrochemical and photophysical as well as their solid state properties.

C.3.1 Synthesis of Alkyne-linked 5NICz

For the synthesis of alkyne-linked 5NICz **XV**, literature known 5NICz (**28**), which has previously been synthesized in our research group following the procedure of Kader et al.,[17] was brominated with NBS in the position 2. To prevent double bromination leading to difficulties in the purification, NBS was added in small portions over a period of 24 h. Br-5NICz (**XIV**) was then reacted in a one-pot double Sonogashira-type reaction with TMS-acetylene (**29**) following the procedure of Qiu et al..[26] The synthesis starting from 5NICz (**28**) is shown in Scheme 21. Purification attempts of alkyne-linked 5NICz (**XV**) *via* recrystallization in several high-boiling solvents like DMSO or nitrobenzene as well as sublimation were not successful. Purification *via* liquid chromatography was not possible due to the low solubility of this system.

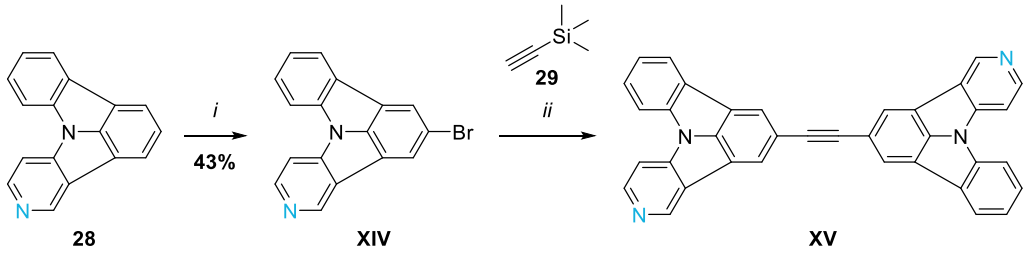

*Scheme 21: Synthesis of alkyne-linked 5NICz **XV***

*i) Bromination of **28**, NBS, MeOH:H_2O, 55 °C; ii) Sonogashira reaction of **XIV** and **29**, Pd(OAc)$_2$, Cu(Xantphos)I, Cs_2CO_3, DMF, 60 °C*

For the one-pot Sonogashira coupling reaction the catalyst Cu(Xantphos)I (**55**) was synthesized according to the procedure of Huang et al.[27] (Scheme 22).

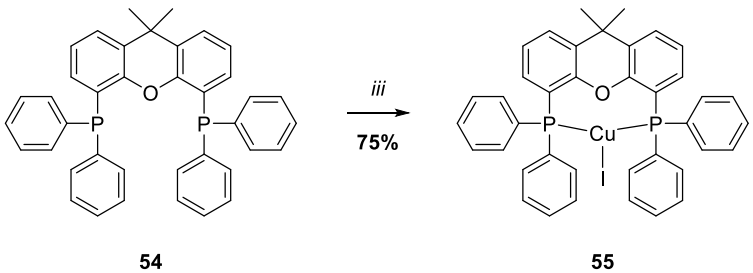

*Scheme 22: Synthesis of Xantphos based catalyst **55***

*iii) **54**, CuI, ACN, 50 °C*

The synthesis was accomplished from readily available Xantphos (**54**) and CuI to give complex **55** in good yield of 75%.

C.3.2 Synthesis of 5,11NICz Building Block for Target Molecule TM2

In the procedure for the synthesis of 5,11NICz reported by Kader et al.[17] starting from 5,11PyCb, which is shown in Scheme 23, the ring closing occurs on the pyridine ring preferentially. Therefore, unsymmetrical 2,5NICz was the main product and 5,11NICz only formed as minor byproduct. Additionally, the two isomers could only be separated by preparative HPLC on rather small scale.

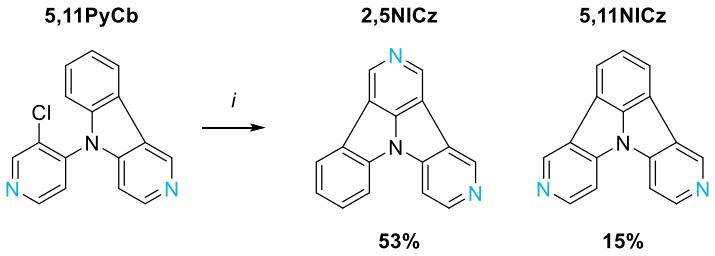

Scheme 23: Synthesis of 5,11NICz as a byproduct
i) CHA of 5,11PyCb, (NHC)Pd(allyl)Cl, K_2CO_3, DMA, 130 °C

Part of this work was the development of a new synthetic route for the selective preparation of 5,11NICz as a building block for the synthesis of molecules like target molecules **TM2**. Two synthetic approaches were considered to selectively form the product, one being the two-sided CHA approach (Scheme 24, a) and the other being the one-sided CHA approach (Scheme 24, b).

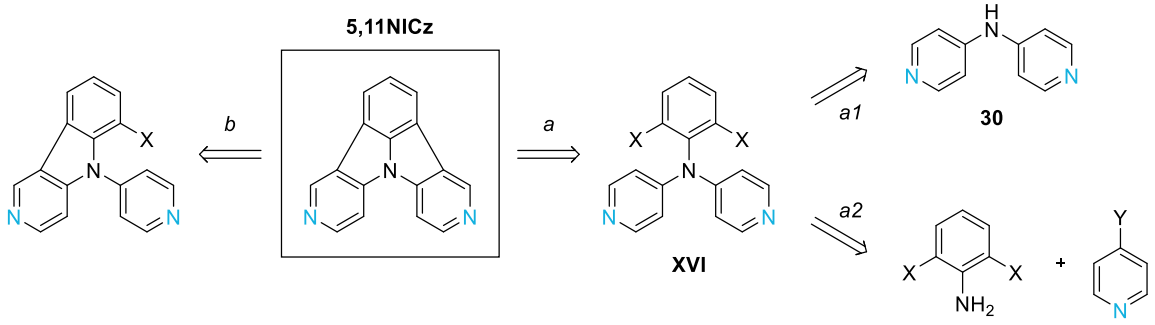

Scheme 24: Synthetic approaches towards 5,11NICz
a) two-sided CHA approach; b) one-sided CHA approach

For the two-sided CHA approach (*a*), two different pathways to synthesize molecule **XVI** were considered, a1 starting from *N*-4-pyridinyl-4-pyridineamine (**30**) and a2 starting from di-halogenated aniline and a pyridine compound.

For pathway a1 starting with **30** and 1,3-dichloro-2-iodobenzene (**31**), which is shown in Scheme 25, different conditions for coupling reactions were tested, but none of them yielded the product **XVI**. The different conditions for the coupling reactions are shown in Table 2.

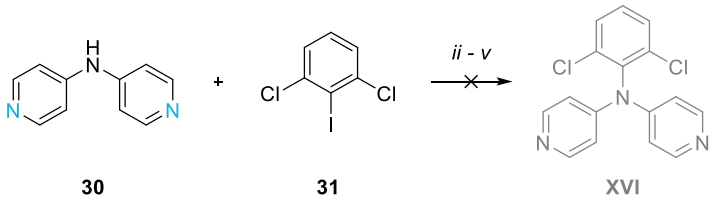

*Scheme 25: Pathway a1 for the synthesis towards **XVI***
*ii – v) Coupling reactions of **30** and **31***

*Table 2: Different conditions for coupling reactions towards compound **XVI***

	Reaction type	Catalyst, Ligand	Base	Solvent	T [°C]
ii	BHA	$Pd(dba)_2$, rac-BINAP (0.04 eq)	NaO^tBu (4 eq)	Toluene	110
iii	BHA	(NHC)Pd(allyl)Cl (0.04 eq)	KO^tBu (4 eq)	DME	84
iv	Ullmann	CuBr (1.2 eq)	Cs_2CO_3 (1.2 eq)	NMP	150
v	Ullmann	$CuSO_4$ (0.19 eq) 18-Crown-6 (0.04 eq)	K_2CO_3 (2 eq)	Ph_2O	180

The formation of **XVI** by nucleophilic substitution failed in previous attempts in our research group, as the pyridine nitrogen atoms reacted preferentially compared to the central nitrogen atom. To overcome this issue, first a methylation of the pyridine nitrogen following the procedure of Bures et al.[28] was performed using iodomethane to form the pyridinium salt **33**, but nucleophilic substitution with 1,3-dichloro-2-fluorobenzene (**34**) failed to form **XVII**. The synthesis is shown in Scheme 26.

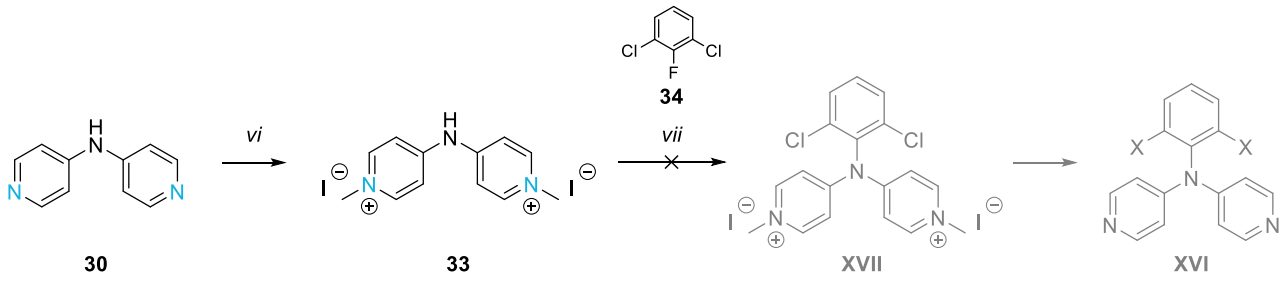

*Scheme 26: Synthesis towards **XVII***
*vi) Methylation of **31**, MeI, rt; vii) S_N reaction of **33** and **34**, Cs_2CO_3, DMF, 130 °C*

Pathway a2 was performed starting with 2,6-dichloroaniline (**35**) and a halogenated pyridine compound, which is shown in Scheme 27. As for the pyridine compounds, 4-iodopyridine (**36**) was commercially available, 4-bromo- (**37**) and 4-chloro-pyridine (**15**) only were available as pyridine hydrochlorides due to limited stability of para halogenated pyridine compounds.

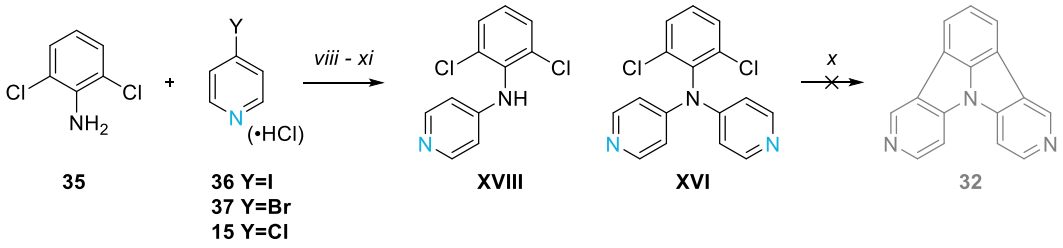

*Scheme 27: Pathway a2 for the synthesis of **XVI***
*viii – xi) Coupling reactions of **35** and **36**/**37**/**15**; x) CHA of **XVIII** and **XVI**, (NHC)Pd(allyl)Cl, K_2CO_3, DMA, 130 °C*

BHA and Ullmann reactions were performed with different conditions, which are shown in Table 3.

*Table 3: Conditions for the synthesis of **XVI***

	Y	Reaction type	Catalyst, Ligand	Base	Solvent	T [°C]	Product
viii	I	BHA	$Pd(dba)_2$, rac-BINAP (0.04 eq)	NaO^tBu (4 eq)	Toluene	110	XVIII + XVI
ix	I	BHA	$Pd(dba)_2$, rac-BINAP (0.04 eq)	Cs_2CO_3 (2.8 eq)	Toluene	110	-
x	Br	Ullmann	CuCl, Phenanthrolin*H_2O (0.1 eq)	KOH (16 eq)	Toluene	110	-
xi	Cl	Ullmann	CuI (0.03 eq)	K_2CO_3 (5 eq)	iPrOH	80	-

Only for conditions *viii*, using $Pd(dba)_2$ and rac-BINAP as catalytic system with sodium *tert*-butoxide as base, product formation together with large amounts of intermediate **XVIII** were observed. Even after a reaction time of several days and addition of additional 4-iodopyridine (**36**) and catalyst to the mixture, the ratio between intermediate and product could not be changed in favor of the product **XVI**. Also, isolation and purification of **XVIII** and performing a second coupling reaction starting from the one-sided product **XVIII** and one equivalent 4-iodopyridine (**36**) failed to form the product. Separation of **XVIII** and **XVI** could only be achieved in a small-scale synthesis (0.7 mmol) with performing MPLC twice followed by preparative HPLC. Attempts to separate the mixture of **XVIII** and **XVI** *via* liquid chromatography and recrystallization on a larger scale were not successful, thus the ring closing *via* CHA was performed using the mixture, however no formation of the product **32** was observed.

Kader et al.[17] reported the use of N-oxides in the synthesis of NICz building blocks, so this strategy was also tested for the synthesis of the 5,11NICz building block **32**, which is shown in Scheme 28.

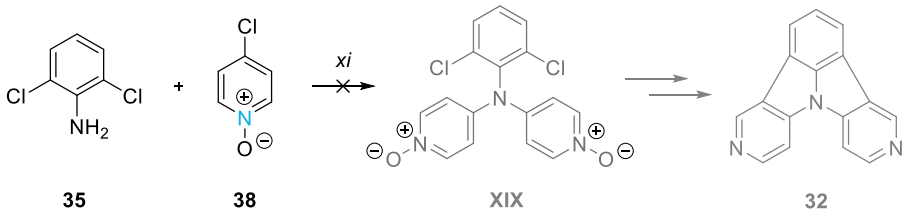

*Scheme 28: Synthesis towards **32** with N-oxides*
*xi) S_N reaction of **35** and **38**, Cs_2CO_3, DMF 130 °C*

Starting with a nucleophilic substitution reaction of 2,6-dichloroaniline (**35**) and 4-chloropyridine N-oxide (**38**), this strategy was unsuccessful to form **XIX** and subsequently the 5,11NICz building block **32**.

The synthetic pathway of the precursor **XXI** for the one-sided CHA approach (*b*) towards the 5,11NICz building block **32** is described in Scheme 29.

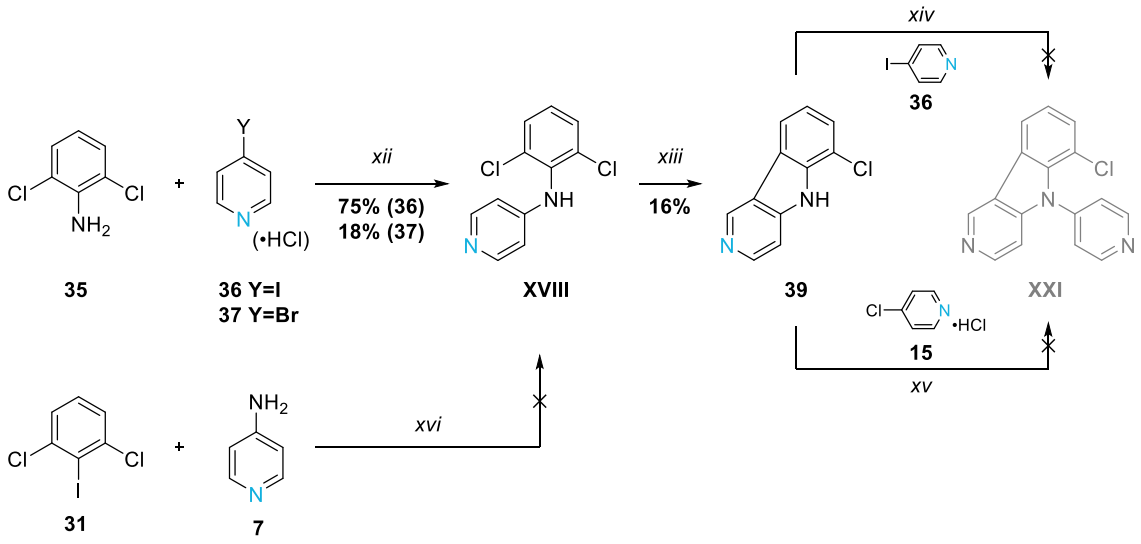

*Scheme 29: Synthesis towards **XXI** via the one-sided CHA approach*
*xii) BHA of **35** and **36**/**37**, $Pd(dba)_2$, rac-BINAP, NaO^{t}Bu, toluene, 110 °C; xiii) CHA of **XVIII**, (NHC)Pd(allyl)Cl, K_2CO_3, DMA, 130 °C; xiv) BHA of **39** and **36**, $Pd(dba)_2$, rac-BINAP, NaO^{t}Bu, toluene, 110 °C; xv) S_N reaction of **39** and **15**, Cs_2CO_3, DMF, 130 °C*

To synthesize molecule **XVIII** two different BHA approaches were performed, one starting with 1,3-dichloro-2-iodobenzene (**31**) and 4-aminopyridine (**7**), which did not yield any product. The other approach starting with 2,6-dichloroaniline (**35**) and 4-iodopyridine (**36**) or 4-bromo-pyridine hydrochloride (**37)** yielded the product **XVIII**. The BHA works with both the 4-iodopyridine (**36**) and the 4-bromo-pyridine hydrochloride (**37**), but with **36** the yield is about four times higher than with **37**. The next step was the ring closing step *via* CHA to form **39**. The low yield is owed to incomplete conversion and several purification steps *via* liquid chromatography and recrystallization. However,

for conversion of **39** using BHA with **36** or nucleophilic substitution employing **15**, no formation of product **XXI** was observed.

C.4 7,9NICz Building Block for Target Molecule TM3

For the synthesis of 7,9NICz several strategies were considered. An overview is shown in Scheme 30. The different strategies being a two-sided CHA, a one-sided CHA, a N-protected CHA, Scholl reaction, photoreaction and a diazotization strategy will be discussed in this chapter.

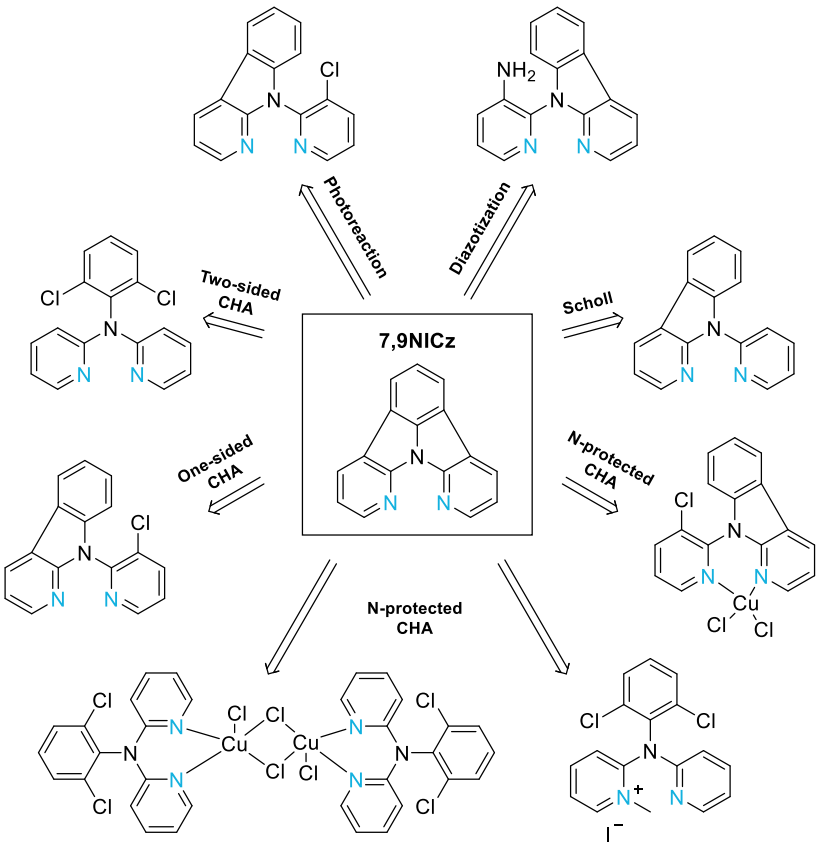

Scheme 30: Strategies for the synthesis of 7,9NICz

C.4.1 Two-sided CHA Strategy

The two-sided CHA strategy was the first and obvious choice to start the synthesis of the 7,9NICz building block, since it is a short and established way to synthesize similar molecules. To synthesize the precursor **XXII**, first a BHA with 2-aminopyridine (**40**) and 2-bromopyridine (**41**) was performed to yield **42** and then a nucleophilic substitution reaction with 1,3-dichloro-2-fluorobenzene (**34**) gave **XXII** in low yields, which is shown in Scheme 31. Also, nucleophilic substitution reaction starting with 2,6-dichloroaniline (**35**) and 2-chloropyridine (**43**) was tested, but this synthesis did not yield the product. BHA starting from 2,6-dichloroaniline (**35**) and 2-bromopyridine (**41**) lead to the product **XXII** in just one step with good yields, however the ring closing CHA did not form the 7,9NICz building block (**44**). A possible explanation for this outcome is the coordination of the Pd catalyst to the two pyridine rings because of the relative positions of the two nitrogen atoms. Nevertheless, to verify this assumption also the one-sided CHA was tested (see chapter C.4.2).

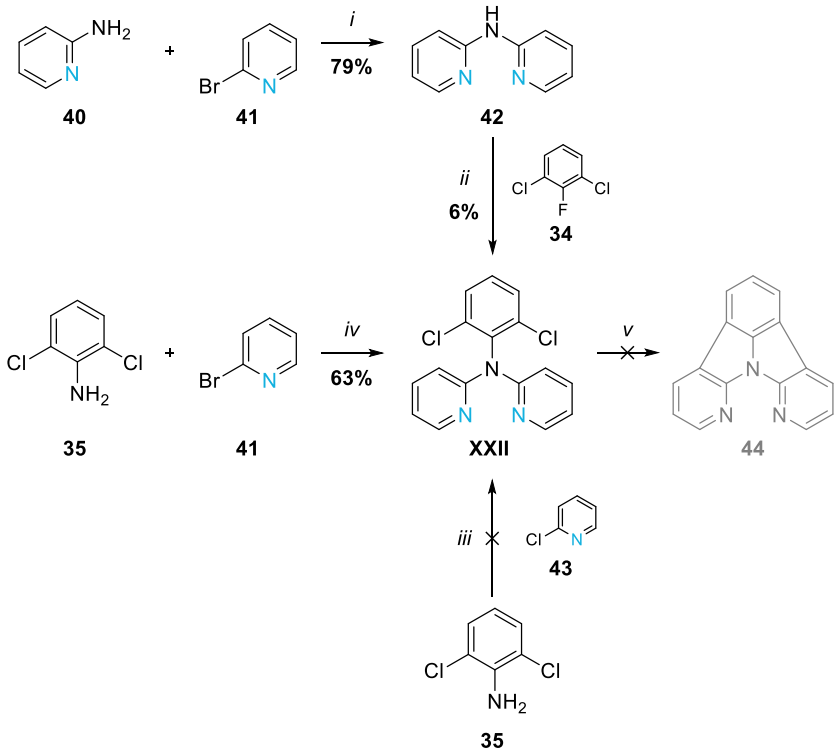

*Scheme 31: Synthesis towards **44***

*i) BHA of **40** and **41**, $Pd_2(dba)_3$, dppf, NaO^{t}Bu, toluene, 110 °C; ii) S_N reaction of **42** and **34**, NaH, DMF, 130 °C; iii) S_N reaction of **35** and **43**, Cs_2CO_3, DMF, 130 °C; iv) BHA of **35** and **41**, $Pd(dba)_2$, rac-BINAP, NaO^{t}Bu, toluene, 110 °C; v) CHA of **XXII**, (NHC)Pd(allyl)Cl, K_2CO_3, DMA, 130 °C*

C.4.2 One-sided CHA Strategy

Since the two-sided CHA strategy did not work for the synthesis of 7,9NICz, a one-sided CHA strategy was considered. The α-carboline (**46**) was synthesized the same way as the γ-carboline by starting with a nucleophilic substitution reaction of benzotriazole (**1**) and 2-bromopyridine (**41**) according to the procedure of Xu et al.,[19] which formed **45** in acceptable yield, followed by a modified Graebe-Ullmann reaction in polyphosphoric acid according to Robinson and Thornley.[20] The synthesis is described in Scheme 32.

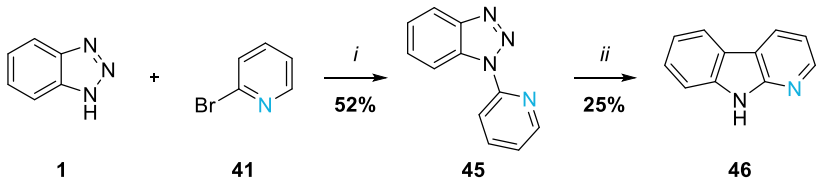

*Scheme 32: Synthesis of **46***

*i) S_N reaction of **1** and **41**, toluene, reflux; ii) Graebe-Ullmann reaction of **45**, polyphosphoric acid, 140 °C*

The precursor **XXIII** for the one-sided CHA strategy was synthesized in good yields *via* nucleophilic substitution of **46** and **47**, which is shown in Scheme 33, however the ring closing CHA to form **44** only yielded the starting material **XXIII**. This supports the earlier assumption, that the pyridine rings of the precursor coordinate to the catalyst. So, the catalyst is irreversible bound to the substrate and therefore no longer available for the ring closing CHA reaction.

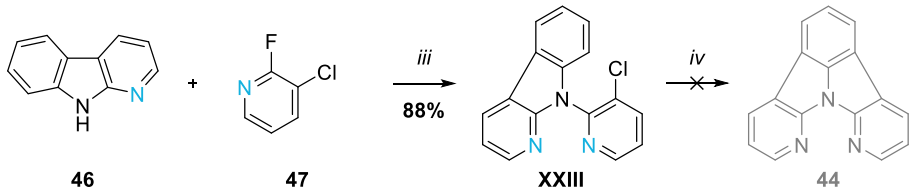

*Scheme 33: Synthesis towards **44***

*iii) S_N reaction of **46** and **47**, Cs_2CO_3, DMF, 130 °C; iv) CHA of **XXIII**, (NHC)Pd(allyl)Cl, K_2CO_3, DMA, 130 °C*

C.4.3 N-protected CHA Strategy

To prevent the catalyst coordination to the precursors **XXII** or **XXIII**, the strategy was to protect one or both nitrogen atoms of the starting materials. Upon protection, the Pd catalyst cannot be consumed by coordination and therefore can act in the ring closing CHA.

First, a N-methylation protocol following the procedure of Bures et al.[28] was performed to yield the N-methyl salt **XXIV**, which was then used for the CHA, but again the ring closing step failed. The synthesis is shown in Scheme 34.

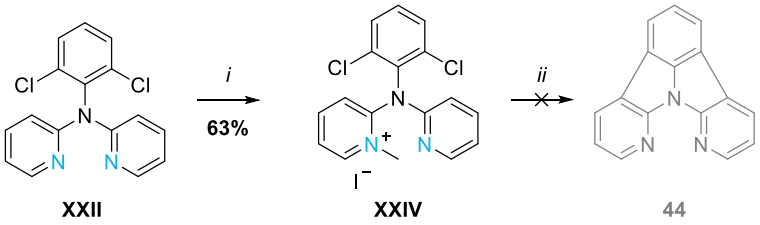

*Scheme 34: Synthesis towards **44***

*i) Methylation of **XXII**, MeI, rt; ii) CHA of **XXIV**, (NHC)Pd(allyl)Cl, K_2CO_3, DMA, 130 °C*

Another workaround was to complex the precursors for the one- and two-sided CHA **XXIII** and **XXII** beforehand and then perform the ring closing CHA with the isolated complexes, which is shown in Scheme 35. However, the CHA also did not yield any product.

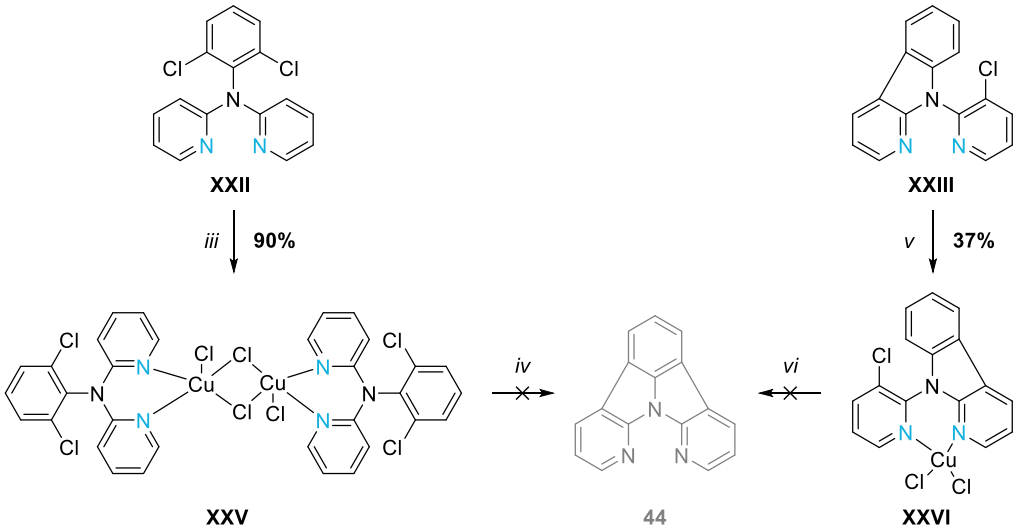

*Scheme 35: Synthesis towards **44** via the N-protected CHA strategy*
*iii) Complexing **XXII**, $CuCl_2$, EtOH, reflux; iv) CHA of **XXV**, (NHC)Pd(allyl)Cl, K_2CO_3, DMA, 130 °C*
*v) Complexing **XXIII**, $CuCl_2$, EtOH, reflux; vi) CHA of **XXVI**, (NHC)Pd(allyl)Cl, K_2CO_3, DMA, 130 °C*

The precursors **XXII** and **XXIII** were reacted with $CuCl_2$ to give the copper complexes **XXV** and **XXVI**, which were isolated and purified by filtration and recrystallization. The molecular structures of **XXV** and **XXVI** are shown in Figure 5 and Figure 6.

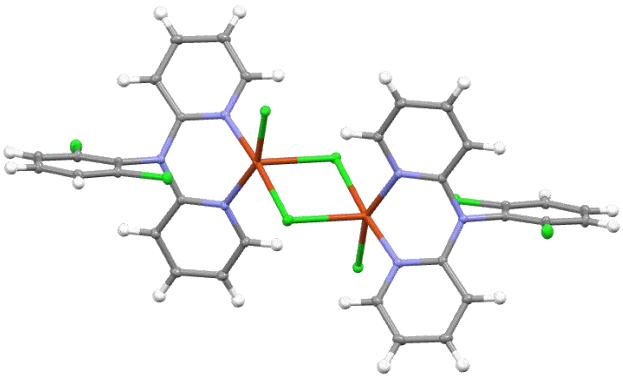

*Figure 5: Molecular structure of **XXV***

Two molecules of **XXII** are connected *via* a $CuCl_2$ bridge, where the copper coordinates between the two nitrogen atoms of the molecule. The dichlorobenzene unit is strongly twisted (80.3°) to the pyridine rings. The pyridine rings, which are connected through the tertiary amine, are almost in a plane (4.4°).

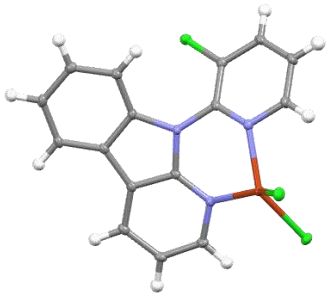

*Figure 6: Molecular structure of **XXVI***

In Figure 6 $CuCl_2$ is only coordinated to one **XXIII** molecule and the chloropyridine unit is slightly rotated out of the plane of the carboline unit in a 41.58 degree angle. However, this strong twist between the chlorobenzene and pyridine or carboline respectively, together with the limited possibility of rotation through the complexation is a possible explanation for the CHA not to work.

C.4.4 Scholl Strategy

Since molecule **48** was obtained as a byproduct from another reaction, a ring closing *via* Scholl reaction protocol following the procedure of Koga et al.[29] with ferric chloride was performed. However, this reaction only gave chlorinated starting material and no formation to the product **44** occurred, which is shown in Scheme 36.

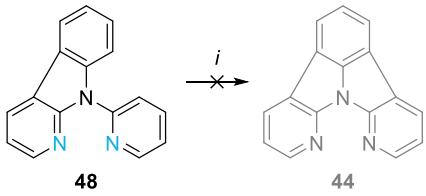

*Scheme 36: Synthesis towards **44** via Scholl strategy*
*i) Scholl reaction of **48**, $FeCl_3$, DCM, 0 °C*

C.4.5 Photoreaction Strategy

Daigle et al.[30] reported a ring closing procedure *via* photochemical cyclodehydrochlorination for molecules similar to **XXIII**. So small tests in 8 mL vials were done with **XXIII** using a 320 nm light source and an optical fiber. Traces of product **44** could be identified *via* GC-MS after one hour. When scaling up the reaction and using a photoreactor with a broader emission spectrum, no reaction occurred, not even after several hours (Scheme 37).

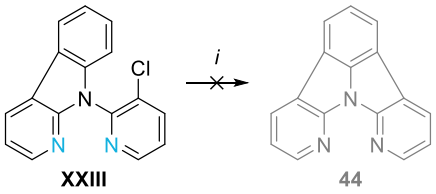

*Scheme 37: Synthesis towards **44** via photoreaction*

*i) Photoreaction of **XXIII**, Na_2CO_3, acetone, rt – 80 °C, hν*

C.4.6 Diazotization Strategy

Since diazotization was already used for the first synthesis of ICz[24] and was part of this work for the synthesis of the test system 2NICz towards **TM1** (see Chapter C.2.4), this strategy was also applied for the synthesis of building block **44**, which is shown in Scheme 38. An advantage of the diazotization strategy in comparison to the CHA strategies is the ring closing without any metal catalyst.

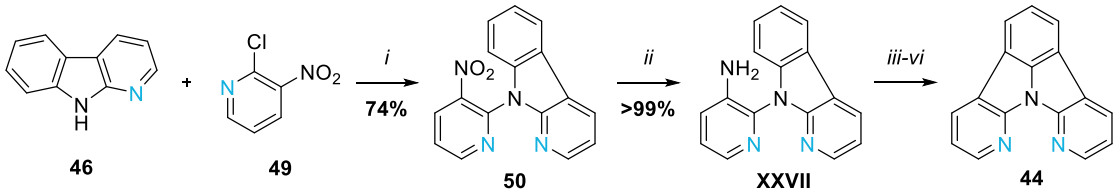

*Scheme 38: Synthesis of **44** via diazotization strategy*

*i) S_N reaction of **46** and **49**, Cs_2CO_3, DMF, 130 °C; ii) Reduction of **50**, $SnCl_2.2H_2O$, EtOH, reflux; iii – vi) Diazotization of **XXVII***

α-Carboline (**46**) and 2-chloro-3-nitropyridine (**49**) were reacted in a nucleophilic substitution reaction to form **50** in good yields and reduction of the nitro group yielded **XXVII** quantitively. The ring closing *via* diazotization reaction was performed using different conditions, which are summarized in Table 4. Reaction *v* and *vi* were performed following the procedure of Choi et al.[31] and Chaturbhuj et al..[32] However, the product **44** could only be obtained with the reaction conditions described in *iii* with a maximum yield of 1%.

*Table 4: Conditions of diazotization reaction of **XXIX** toward building block **44***

	Reagents	Solvent	T [°C]	Yield
iii	$NaNO_2$	AcOH, H_2SO_4, H_2O	0 - 90	**1%**
iv	$NaNO_2$, Cu	AcOH, H_2SO_4, H_2O	0 - 90	**traces**
v	Isoamyl nitrite	ACN	rt - 80	-
vi	Isoamyl nitrite, TEOF	DMF	rt - 80	-

C.5 Summary and Outlook

The incorporation of NICz building blocks in larger systems with different positioning of the nitrogen atoms as well as the synthetic pathways towards different NICz building blocks were investigated. Target molecule **TM1** was successfully synthesized. However, three structural isomers were formed due to the position of the functional groups on the free rotatable benzene ring. Because of poor solubility, this mixture could not be separated *via* liquid chromatography or recrystallization. For increasing solubility of this system, butyl chains were attached to the pyridine nitrogen to form a pyridinium salt. Unfortunately, the solubility was still not high enough to achieve separation *via* preparative HPLC, but analytic tests showed a promising separation of three compounds. Additional investigations will be done by attaching longer alkyl chains to further increase the solubility of these pyridinium salts. After successful separation of the three structural isomers, crystal growth and electrochemical and photophysical characterization of **TM1** will be performed to investigate the influence of the non-classical C-H···N hydrogen bonds.

The synthesis of large molecules like target molecule **TM2** using previously established NICz building blocks was investigated. Therefore, the alkyne-linked 5NICz was successfully synthesized starting from 5NICz *via* a one-pot Sonogashira coupling reaction. Due to low solubility of this system, purification was problematic. Further purification attempts performing crystallization will be tried in the future. Also, forming pyridinium salts by attaching alkyl chains is a possible strategy for purification. The necessary building block **5,11NICz** for the synthesis of an additional large system could not be prepared.

The building block **7,9NICz** for self-assembly investigations was synthesized *via* the diazotization approach, but only in poor yields. Other approaches like the CHA or the N-protected CHA strategy failed to form this building block, probably due to the coordination of the metal ion of the catalyst between the two nitrogen atoms. Nevertheless, the observations of the strong affinity of these substrates to coordinate to different metals underlines why especially this NICz building block is of great interest. To increase the yield of the diazotization approach, adjustments on the reaction conditions are necessary. Next steps for the synthesis of **TM3** will be the functionalization of **7,9NICz** in the position 2 and a subsequent coupling reaction. Lastly, the self-assembly properties of **TM3** will be investigated.

D. Experimental Part

D.1 General Remarks

Unless explicitly mentioned otherwise, all reagents from commercial suppliers were used without further purification. Absolute, anhydrous solvents like toluene were absolutized by the *PURESOLV*-system from Innovative Technology Inc. Other commercially available solvents like DMA or DMF were purchased from commercial suppliers. The commercially available lithiation reagent *n*-BuLi was used without additional quantitative analysis, using the declared value.

D.2 Chromatographic Methods

D.2.1 Thin Layer Chromatography

Thin layer chromatography (TLC) was performed using TLC-aluminum foil (Merck, silica 60, F254).

D.2.2 Column Chromatography

Preparative column chromatography was performed using a *BÜCHI SepacoreTM* flash system, which was equipped with the following components:

- Pump system: 2 *BÜCHI* pump modules C-605
  BÜCHI pump manager C-615
- Detector: *BÜCHI* UV photometer C-635
- Fraction collector: *BÜCHI* fraction collector C-660

The appropriate PP-cartridges were packed with silica gel (Merck, 40-63 µm).

D.2.3 Sublimation

For purification a self-made, turbomolecular-supported high vacuum sublimation system with following components was used:

- Pump system: *Leybold Turbovac 50* turbomolecular pump
  Rotary vacuum pump
- Oven: *BÜCHI* glass oven B-585
- Cold trap: filled with liquid nitrogen
- Pressure sensor: Balzers PKR 250 gauge
  Balzers TPG 251 control unit

D.3 Analytic Methods

D.3.1 NMR Spectroscopy

NMR spectra were recorded using a Bruker Avance DRX400 MHz (400 MHz for ^{1}H; 100 MHz for ^{13}C) or DRX-600 MHz (600 MHz for ^{1}H; 150 MHz for ^{13}C) Fourier transform spectrometer. ^{1}H- and ^{13}C-spectra are given as stated: chemical shift in parts per million (ppm) referenced to the according solvent (^{1}H: $CDCl_3$ δ=7.26 ppm, CD_2Cl_2 δ=5.32 ppm, DMSO-d6 δ=2.50 ppm; ^{13}C: $CDCl_3$ δ=77.0 ppm, CD_2Cl_2 δ=54.0 ppm, DMSO-d6 δ=39.5 ppm) with tetramethylsilane (TMS) at δ=0 ppm. Multiplicities of the signals are given as: ^{1}H: s=singlet, d=doublet, t=triplet and m=multiplet.

D.3.2 GC-MS Measurements

GC-MS measurements were conducted using GC-MS interface from *Thermo Scientific™*:

- *TRACE™* 1300 gas chromatograph with a *Restek® Rxi®-5Sil MS column (l=30 m, ID = 0.25 mm, 0.25 µm film, achiral)*
- *ISQ™ LT single quadrupole mass spectrometer (EI = electron ionization)*

D.3.3 Single Crystal Diffraction

Single crystal structures were determined in collaboration with Dr. Berthold Stöger and the X-ray centre. All data were collected on an *APEX* II diffractometer with κ geometry, equipped with a CCD detector using Mo *K*α irradiation at 100 K in a dry stream of nitrogen.

D.4 Synthesis and Characterization of the Compounds

Detailed experimental procedures for the synthesis of each compound as well as their characterization are presented in the following chapter.

D.4.1 Synthesis of Target Molecule TM1

D.4.1.1 1-(3-Bromo-4-pyridinyl)-1H-benzotriazole (3)

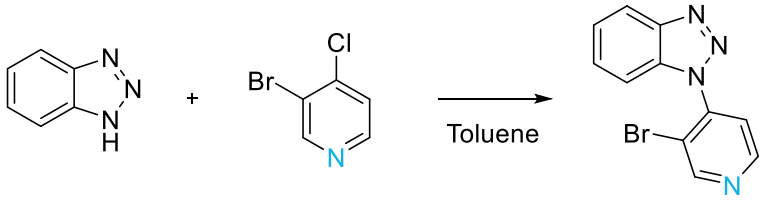

1 **2** **3**

Synthesis of **3** was done according to Xu et al.[19]

1*H*-Benzotriazole **1** (2 eq, 32 mmol, 3.813 g) and 3-bromo-4-chloropyridine **2** (1 eq, 16 mmol, 3.089 g) were dissolved in 16 mL anhydrous toluene and heated to reflux. After 21 h the reaction was cooled to room temperature, poured on 2N NaOH and extracted with EE three times. The combined organic layers were washed with saturated NaCl solution, dried over Na_2SO_4 and concentrated under reduced pressure. Recrystallization from EtOH yielded **3** (3.570 g, 13 mmol, 41%) as white solid.

^{1}H NMR (400 MHz, $CDCl_3$, FID BIM128/20) δ = 9.06 (s, 1H), 8.79 (d, J = 5.1 Hz, 1H), 8.20 (dt, J = 8.4, 1.0 Hz, 1H), 7.60 (ddd, J = 8.2, 7.0, 1.1 Hz, 1H), 7.55 (d, J = 5.1 Hz, 1H), 7.53 – 7.42 (m, 2H) ppm.

D.4.1.2 4-Bromo-5H-pyrido[4,3-b]indole (4)

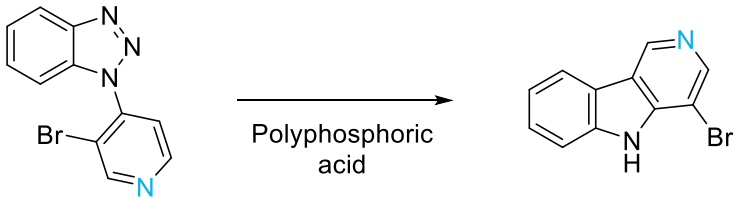

3 **4**

Synthesis of **4** followed the procedure according to Robinson and Thornley.[20]

Polyphosphoric acid (20 eq, 73 mmol, 7.134 g) was mixed with **3** (1 eq, 3.7 mmol, 1.001 g) in a three-necked flask, heated to 170 °C slowly and stirred for about 5 h. The reaction was cooled to 110 °C and 50 mL H_2O were added. After cooling to room temperature, the reaction mixture was neutralized

with 2N NaOH and stirred for 10 min. The resulting solid was filtered and dried to give **4** (341 mg, 1.38 mmol, 38%) as white solid.

^{1}H NMR (400 MHz, $CDCl_3$, FID BIM141/10) δ = 9.23 (s, 1H), 8.70 (s, 1H), 8.62 (s, 1H), 8.14 (d, J = 7.9 Hz, 1H), 7.61 – 7.53 (m, 2H), 7.40 (ddd, J = 8.1, 6.4, 1.8 Hz, 1H) ppm.

D.4.1.3 3-Chloro-4-pyridinamine (8)

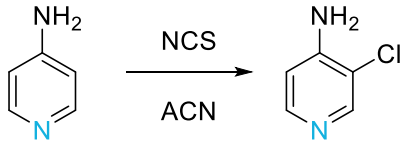

7 **8**

4-Pyridinamine **7** (1 eq, 50 mmol, 4.710 g) was dissolved in 250 mL ACN. While stirring, NCS (1.2 eq, 60 mmol, 8.010 g) was added in small portions whereby the solution turned from colorless to orange. After stirring for four days at room temperature, the solvent was evaporated under reduced pressure. The residue was dissolved in diethyl ether and extracted with 2N NaOH. The combined organic layers were washed with 2N NaOH three times, dried over Na_2SO_4, filtered and the solvent was evaporated under reduced pressure. The crude product was purified *via* flash chromatography (LP:EE 75%) to yield **8** (637 mg, 5 mmol, 10%) as orange crystals.

^{1}H NMR (400 MHz, $CDCl_3$, FID BIM102/30) δ = 8.29 (s, 1H), 8.10 (d, *J* = 5.5 Hz, 1H), 6.62 (d, *J* = 5.5 Hz, 1H), 4.63 (s, 2H) ppm.

D.4.1.4 N-(2-Bromophenyl)-3-chloro-4-pyridinamine (10)

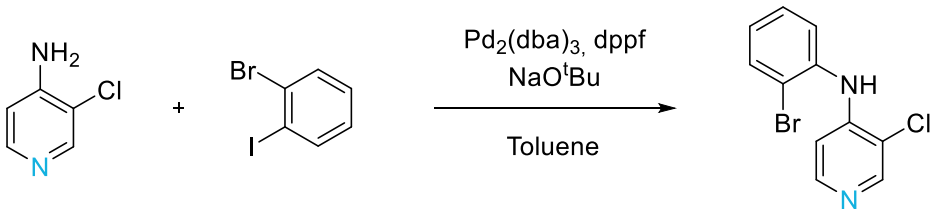

8 **9** **10**

4-Amino-3-chloropyridine **8** (1 eq, 2 mmol, 257 mg), 2-bromoiodobenzene **9** (1.2 eq, 2.4 mmol, 679 mg), $Pd_2(dba)_3$ (0.02 eq, 0.04 mmol, 37 mg), dppf (0.04 eq, 0.08 mmol, 44 mg) and NaO^tBu (1.4 eq, 2.8 mmol, 271 mg) were dissolved in 12 mL anhydrous, degassed toluene and stirred 23 h at 110 °C under argon atmosphere. The reaction mixture was flashed over celite and the crude product was purified *via* column chromatography (LP:EE 16 → 20%) to yield **10** (536 mg, 1.9 mmol, 95%) as brown solid.

^{1}H NMR (400 MHz, $CDCl_3$, FID BIM119/30) δ = 8.45 (s, 1H), 8.19 (s, 1H), 7.69 (dd, J = 8.0, 1.4 Hz, 1H), 7.45 (d, J = 7.2 Hz, 1H), 7.37 (t, J = 7.6 Hz, 1H), 7.10 (t, J = 7.6 Hz, 1H), 6.95 (bs, 1H), 6.79 (bs, 1H) ppm.

^{13}C NMR (101 MHz, $CDCl_3$, FID BIM119/51) δ = 149.4, 148.6, 146.0, 137.1, 133.8, 128.5, 126.2, 123.2, 118.6, 117.9, 107.9 ppm.

D.4.1.5 4-Chloro-5H-pyrido[4,3-b]indole (11)

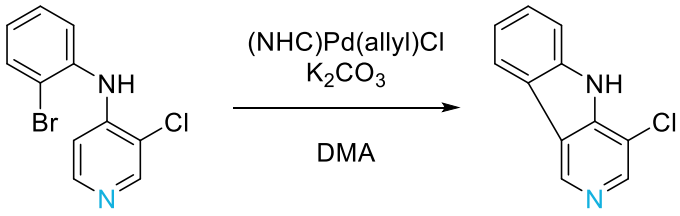

10 **11**

10 (1 eq, 0.7 mmol, 199 mg), (NHC)Pd(allyl)Cl **53** (0.1 eq, 0.07 mmol, 40 mg) and K_2CO_3 (2 eq, 1.4 mmol, 207 mg) were suspended in 7 mL degassed DMA under argon atmosphere and heated to 130 °C for seven days. After cooling to room temperature, the suspension was diluted with H_2O and extracted with DCM three times. The combined organic layers were dried over Na_2SO_4, filtrated and the solvent was removed under reduced pressure. Purification *via* column chromatography (13 g SG, LP:EE 25%) yielded a mixture of starting material **10** and product **11** (68,4 mg).

D.4.1.6 2,5-Dibromo-N^1,N^4-bis-4-(3-chloropyridinyl)benzene-1,4-diamine (III)

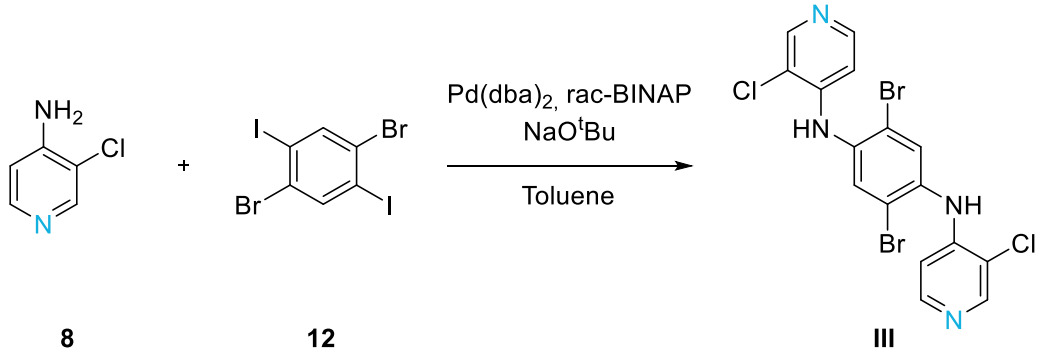

8 **12** **III**

1,4-Dibromo-2,5-diiodobenzene **12** (1 eq, 0.8 mmol, 401 mg), 4-amino-3-chloropyridine **8** (2.2 eq, 1.8 mmol, 234 mg), $Pd(dba)_2$ (0.04 eq, 0.03 mmol, 20 mg), rac-BINAP (0.04 eq, 0.03 mmol, 21 mg) and NaO^tBu (4 eq, 3.3 mmol, 320 mg) were dissolved in 3 mL anhydrous, degassed toluene under argon atmosphere and light exclusion and heated to 110 °C. After 20 days the reaction mixture was cooled to room temperature, poured onto H_2O and extracted with DCM three times. The combined organic layers were washed with H_2O, dried over Na_2SO_4 and the solvent was removed under reduced pressure. The crude product was purified *via* column chromatography (DCM:MeOH 1 →

10%) and afterwards washed with about 10 mL cooled DCM to remove residues of starting material **8** to give **III** (58 mg, 0.12 mmol, 14%) as white solid.

^{1}H NMR (400 MHz, DMSO-d6, FID BIM190/60) δ = 8.40 (s, 2H), 8.36 (s, 2H), 8.12 (d, J = 5.6 Hz, 2H), 7.80 (s, 2H), 6.47 (d, J = 5.6 Hz, 2H) ppm.

^{13}C NMR (101 MHz, DMSO-d6, FID BIM190/63) δ = 148.6, 148.3, 147.2, 137.0, 132.8, 121.0, 116.7, 109.0 ppm.

D.4.1.7 1,4-Dibromo-2,5-dichlorobenzene (14)

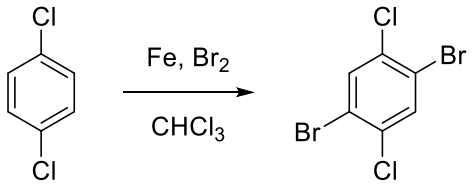

13 **14**

Synthesis of **14** was performed according to the procedure of Lai et al.[22]

1,4-Dichlorobenzene **13** (1 eq, 28 mmol, 4.2 g) and Fe-powder (0.15 eq, 4 mmol, 0.24 g) were suspended in 15 mL chloroform. Br_2 (2.35 eq, 67 mmol, 10.9 g) was added dropwise to the reaction mixture and stirred for 22 h at room temperature. Sodium thiosulfate solution was added, and the solution was extracted with DCM three times. The combined organic layers were washed with H_2O, dried over Na_2SO_4, filtrated and the solvent was evaporated under reduced pressure. Purification *via* recrystallization from ethanol yielded **14** (4.7 g, 15.4 mmol, 54%) as white needles.

^{1}H NMR (400 MHz, $CDCl_3$, FID BIM229/20) δ = 7.71 (s, 2H) ppm.

D.4.1.8 1-(4-Pyridinyl)-1H-benzotriazole (16)

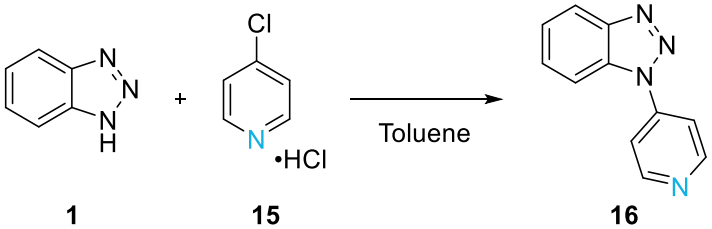

1 **15** **16**

Synthesis of **16** was done according to Xu et al.[19]

1*H*-Benzotriazole **1** (2 eq, 120 mmol, 14.3 g) and 4-chloropyridine hydrochloride **15** (1 eq, 60 mmol, 9.0 g) were suspended in 60 mL anhydrous toluene under argon atmosphere and stirred at 110 °C for 19 h. The cooled reaction mixture was suspended in 2N NaOH and extracted with EE three times. The combined organic layers were washed with H_2O, dried over Na_2SO_4, filtrated and the solvent

was removed under reduced pressure. The crude product was recrystallized from cyclohexane to give **16** (12.0 g, 60 mmol, quant.) as white solid.

^{1}H NMR (400 MHz, $CDCl_3$, FID BIM238/20) δ = 8.91 – 8.84 (m, 2H), 8.21 (dt, J = 8.3, 1.0 Hz, 1H), 7.92 – 7.86 (m, 3H), 7.66 (ddd, J = 8.3, 7.0, 1.1 Hz, 1H), 7.51 (ddd, J = 8.1, 7.0, 1.0 Hz, 1H) ppm.

D.4.1.9 5H-Pyrido[4,3-b]indole (18)

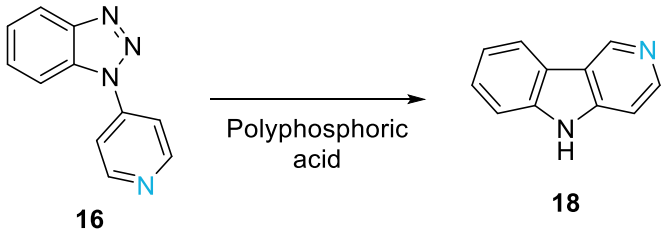

16 **18**

Synthesis of **18** followed the procedure according to Robinson and Thornley.[20]

16 (1 eq, 61 mmol, 11.95 g) and polyphosphoric acid (16 eq, 976 mmol, 95 g) were heated to 140 °C in a three-necked flask for about 8 h. After cooling to room temperature, the reaction mixture was diluted with H_2O and the brown precipitate was filtered off. 4N NaOH was added to the filtrate to give basic conditions. The white solid was filtered off, washed with H_2O and dried under reduced pressure to give **18** (4.92 g, 29 mmol, 48%) as off-white solid.

^{1}H NMR (400 MHz, DMSO-d6, FID BIM242/10) δ = 11.70 (s, 1H), 9.33 (s, 1H), 8.41 (d, J = 5.7 Hz, 1H), 8.22 (dt, J = 7.8, 1.0 Hz, 1H), 7.56 (dt, J = 8.2, 0.9 Hz, 1H), 7.50 – 7.43 (m, 2H), 7.26 (ddd, J = 8.1, 7.1, 1.1 Hz, 1H) ppm.

D.4.1.10 N-(2-Bromophenyl)-4-pyridinamine (17)

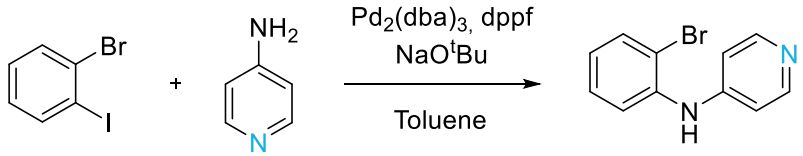

9 **7** **17**

4-Pyridinamine **7** (1 eq, 20 mmol, 1.88 g), $Pd_2(dba)_3$ (0.01 eq, 0.2 mmol, 190 mg), dppf (0.06 eq, 1.2 mmol, 667 mg) and NaO^tBu (1.4 eq, 28 mmol, 2.7 g) were dissolved in 80 mL anhydrous, degassed toluene under argon atmosphere. After addition of 1-bromo-2-iodobenzene **9** (1.2 eq, 24 mmol, 6.82 g) under argon counterflow, the reaction mixture was heated to reflux until full conversion (TLC). The mixture was cooled to room temperature, filtrated over celite and washed with EE. After removing the solvent under reduced pressure, the crude product was purified *via* column chromatography (DCM:MeOH 1%) to give **17** (2.67 g, 10.7 mmol, 54%) as brown solid.

^{1}H NMR (400 MHz, $CDCl_3$, FID BIM191/30) δ = 8.40 – 8.32 (m, 2H), 7.62 (dd, J = 8.0, 1.5 Hz, 1H), 7.46 (dd, J = 8.1, 1.6 Hz, 1H), 7.34 – 7.27 (m, 1H), 6.97 (ddd, J = 8.0, 7.3, 1.6 Hz, 1H), 6.91 – 6.86 (m, 2H), 6.20 (bs, 1H) ppm.

D.4.1.11 5H-Pyrido[4,3-b]indole (18)

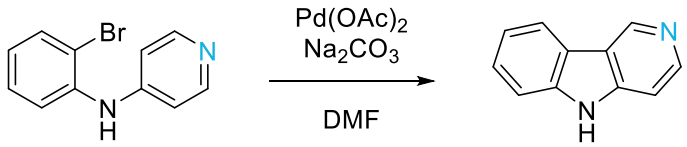

17 **18**

$Pd(OAc)_2$ (0.1 eq, 0.2 mmol, 43 mg) and Na_2CO_3 (1.4 eq, 2.7 mmol, 289 mg) were placed in a glass vial. **17** (1 eq, 1.9 mmol, 477 mg) was dissolved in 10 mL degassed DMF and added to the glass vial under argon atmosphere. The reaction mixture was heated to 160 °C until full conversion (GC-MS). The solution was cooled to room temperature, filtrated over celite and washed with EE. The solution was extracted with saturated NaCl solution three times. The combined organic layers were washed with H_2O, dried over Na_2SO_4 and the solvent was removed under reduced pressure. The crude product was recrystallized from toluene to give **18** (136 mg, 0.8 mmol, 42%) as brown crystals.

^{1}H NMR (400 MHz, DMSO-d6, FID BIM207/20) δ = 11.70 (s, 1H), 9.33 (s, 1H), 8.41 (d, J = 5.7 Hz, 1H), 8.22 (dd, J = 7.8, 1.1 Hz, 1H), 7.56 (dt, J = 8.2, 0.9 Hz, 1H), 7.50 – 7.44 (m, 2H), 7.26 (ddd, J = 8.0, 7.1, 1.1 Hz, 1H) ppm.

D.4.1.12 5,5'-(1,4-(2,5-Dibromo)phenylene))-bis-5H-pyrido[4,3-b]indole (VI)

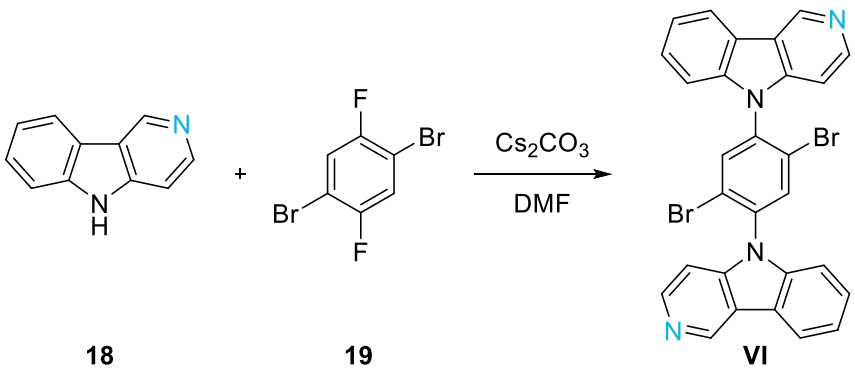

18 **19** **VI**

18 (2 eq, 12 mmol, 2.03 g), 1,4-dibromo-2,5-difluorobenzene **19** (1 eq, 6 mmol, 1.64 g) and Cs_2CO_3 (2.2 eq, 13.2 mmol, 4.33 g) were dissolved in 12 mL DMF under argon atmosphere, heated to 130 °C and stirred overnight. The cooled reaction mixture was diluted in DCM and H_2O. After phase separation, the aqueous phase was extracted with DCM three times and the combined organic layers were washed with H_2O. After drying over Na_2SO_4, the solvent was removed under reduced pressure.

The crude product was purified *via* column chromatography (DCM:MeOH 1%) to give **VI** as two different rotamers (overall 2.32 g, 4 mmol, 70%) as brown solid.

^{1}H NMR (400 MHz, DMSO-d6, FID BIM227/60) δ = 9.52 (s, 2H), 8.57 (d, J = 5.7 Hz, 2H), 8.47 (s, 2H), 8.41 (dt, J = 7.8, 1.0 Hz, 2H), 7.59 (ddd, J = 8.3, 7.1, 1.2 Hz, 2H), 7.53 – 7.42 (m, 6H) ppm.

^{13}C NMR (101 MHz, DMSO-d6, FID BIM227/63) δ = 145.4, 144.3, 143.0, 140.3, 136.9, 136.0, 127.3, 123.1, 121.6, 121.0, 119.5, 110.8, 105.8 ppm.

^{1}H NMR (400 MHz, $CDCl_3$, FID BIM227/70) δ = 9.45 (s, 2H), 8.63 (d, J = 5.6 Hz, 2H), 8.27 (dt, J = 7.8, 1.0 Hz, 2H), 8.04 (s, 2H), 7.58 (ddd, J = 8.3, 7.2, 1.2 Hz, 2H), 7.47 (ddd, J = 8.1, 7.3, 1.0 Hz, 2H), 7.29 (dt, J = 8.2, 0.9 Hz, 2H), 7.19 (dd, J = 5.7, 1.0 Hz, 2H) ppm.

^{13}C NMR (101 MHz, $CDCl_3$, FID BIM227/73) δ = 146.0, 144.7, 143.4, 140.4, 137.8, 135.9, 127.6, 123.2, 122.3, 122.0, 121.2, 120.5, 110.5, 105.5 ppm.

D.4.1.13 Benzo[1,2-b:4,5-b']dibenzo[e:e']dipyrido[3'',4'',5''-gh:3''',4''',5'''-g'h']dipyrrolizine (TM1)

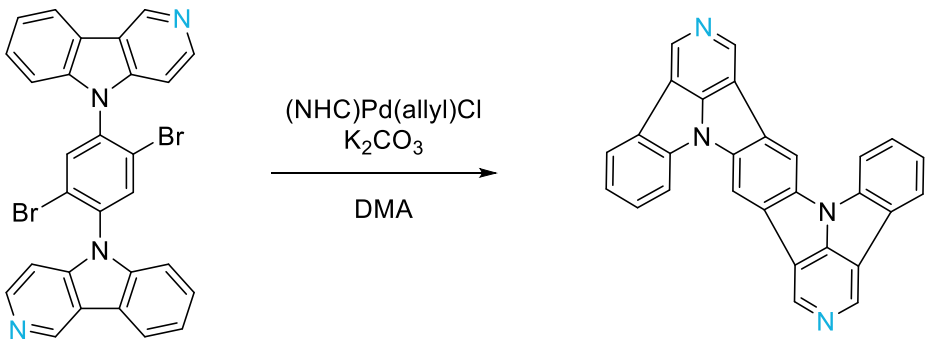

VI **TM1**

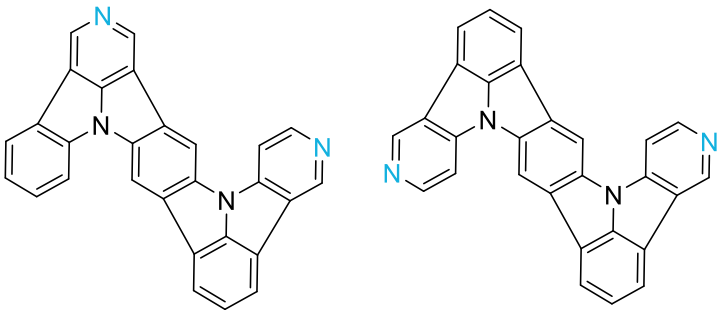

VII **VIII**

VI (1 eq, 0.95 mmol, 542 mg), (NHC)Pd(allyl)Cl **53** (0.05 eq, 0.048 mmol, 27 mg) and K_2CO_3 (2 eq, 1.91 mmol, 264 mg) were suspended in 10 mL degassed DMA under argon atmosphere and heated to 130 °C for 24 h. After cooling to room temperature, the green solid was filtrated, washed with chloroform and dried under reduced pressure. For purification the crude product was heated to reflux in DMSO for several hours, filtrated, washed with chloroform, methanol and DCM and dried under reduced pressure to give a mixture of **TM1**, **VII** and **VIII** (overall 402 mg, quant.).

D.4.1.14 Benzo[1‘‘‘,2‘‘‘-2,3:4‘‘‘,5‘‘‘-2‘,3‘]dibenzo[4,5:4‘‘,5‘‘]dipyrrolizido[6,6a,1-c,d:6‘,6a‘,1‘-c‘,d‘]di(1-butyl)pyridiniumdiiodide (IX)

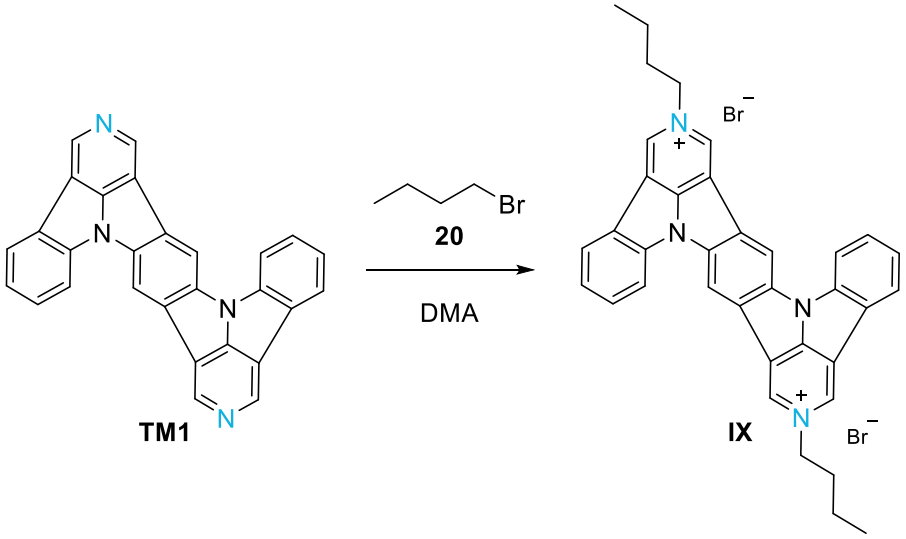

TM1[a] (1 eq, 0.94 mmol, 384 mg) and 1-bromobutane **20** (20 eq, 19 mmol, 2 mL) were suspended in 15 mL DMA and heated to 150 °C for four days. After removing the solvent under reduced pressure, the crude product was suspended in warm methanol. The solid was separated from the solvent *via* centrifugation and dried under reduced pressure. Analytical separation *via* HPLC (MeOH/water) was performed by dissolving the crude product in methanol. For preparative separation *via* HPLC the solubility was too low.

[a] TM1 as a mixture with VII and VIIII

D.4.1.15 5-(2-Nitrophenyl)-5H-pyrido[4,3-b]indole (X)

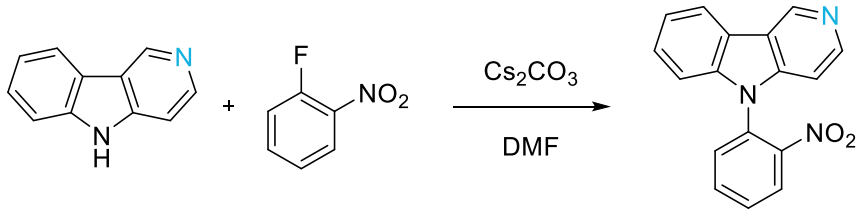

18 **21** **X**

γ-Carboline **18** (1 eq, 0.7 mmol, 117 mg), 1-fluoro-2-nitrobenzene **21** (1.2 eq, 0.8 mmol, 120 mg) and Cs_2CO_3 (1.2 eq, 0.8 mmol, 272 mg) were stirred in 1.4 mL DMF at 130 °C until full conversion (TLC). The reaction mixture was poured on H_2O, extracted with DCM three times, dried over Na_2SO_4 and the solvent was removed under reduced pressure. The crude product was purified *via* column chromatography (DCM:MeOH 1 → 10%) to give **X** (57.8 mg, 0.2 mmol, 29 %) as yellow solid.

^{1}H NMR (400 MHz, $CDCl_3$, FID BIM175/20) δ = 9.39 (s, 1H), 8.53 (d, J = 5.8 Hz, 1H), 8.23 (dd, J = 10.9, 8.3 Hz, 2H), 7.91 (t, J = 7.5 Hz, 1H), 7.78 (t, J = 7.7 Hz, 1H), 7.67 (d, J = 7.8 Hz, 1H), 7.48 (t, J = 7.7 Hz, 1H), 7.41 (t, J = 7.5 Hz, 1H), 7.13 (d, J = 8.1 Hz, 1H), 7.06 (d, J = 5.7 Hz, 1H) ppm.

D.4.1.16 5-(2-Aminophenyl)-5H-pyrido[4,3-b]indole (XI)

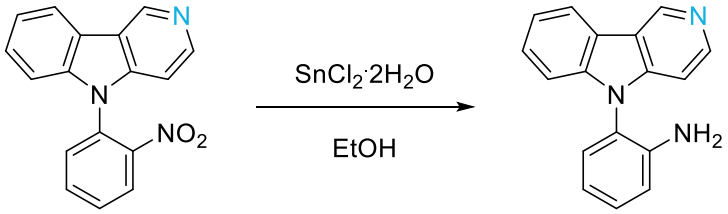

X **XI**

X (1 eq, 0.2 mmol, 58 mg) and $SnCl_2{\cdot}2H_2O$ (3.5 eq, 0.7 mmol, 186 mg) were heated to reflux in 1 mL EtOH and stirred until full conversion (GC-MS). The reaction mixture was cooled to room temperature and poured onto H_2O. 2N NaOH was added until basic conditions. The aqueous solution was extracted with DCM, the combined organic layers were washed with H_2O, dried over Na_2SO_4 and the solvent was removed under reduced pressure to give **XI** (47 mg, 0.18 mmol, 91%) as yellow solid.

^{1}H NMR (400 MHz, $CDCl_3$, FID BIM178/10) δ = 9.39 (s, 1H), 8.52 (d, J = 5.8 Hz, 1H), 8.23 (d, J = 7.8 Hz, 1H), 7.54 – 7.45 (m, 1H), 7.43 – 7.33 (m, 2H), 7.24 (d, J = 6.0 Hz, 2H), 7.13 (d, J = 5.7 Hz, 1H), 6.99 (dd, J = 8.1, 1.4 Hz, 1H), 6.94 (td, J = 7.6, 1.4 Hz, 1H), 3.54 (s, 2H) ppm.

D.4.1.17 Dibenzo[b,e]pyrido[3,4,5-gh]pyrrolizine (22)

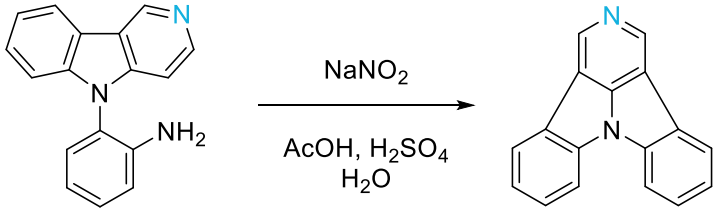

XI **22**

XI (1 eq, 0.2 mmol, 47 mg) was dissolved in 0.5 mL acetic acid and 0.1 mL conc. sulfuric acid and cooled to 0 °C. Sodium nitrite (1.1 eq, 0.2 mmol, 14 mg) was dissolved in 0.3 mL H_2O and added dropwise to the reaction mixture. After 10 min at 0 °C, the reaction mixture was stirred at room temperature for 1 h and then heated to 98 °C overnight. The reaction mixture was cooled to room temperature, poured onto H_2O and 2N NaOH was added to give basic conditions. After extraction with DCM, the combined organic layers were washed with H_2O, dried over Na_2SO_4 and the solvent was removed under reduced pressure. For characterization TLC with a reference and GC-MS were performed.

D.4.1.18 N-(2,5-Difluorophenyl)acetamide (25)

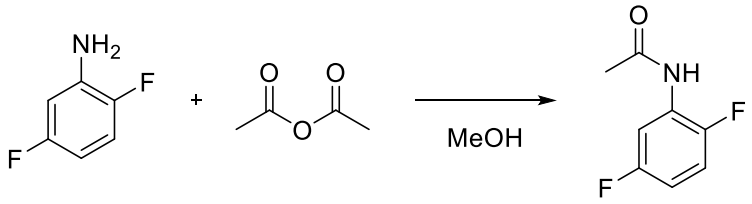

23 **24** **25**

2,5-Difluoroaniline **23** (1 eq, 24 mmol, 3.1 g) and acetic anhydride **24** (5 eq, 120 mmol, 12 mL) were dissolved in 80 mL MeOH and heated to reflux for 30 minutes. After cooling to room temperature, the solvent was removed under reduced pressure. The liquid was poured on ice water and stirred for 3 h. The white solid was filtered off, washed with H_2O and dried to give **25** (2.65 g, 15.4 mmol, 64%) as white solid.

^{1}H NMR (400 MHz, $CDCl_3$, FID BIM186/20) δ = 8.17 (ddd, J = 10.0, 6.3, 3.2 Hz, 1H), 7.42 (bs, 1H), 7.02 (ddd, J = 10.4, 9.0, 4.9 Hz, 1H), 6.71 (ddt, J = 9.0, 7.4, 3.6 Hz, 1H), 2.23 (s, 3H) ppm.

D.4.1.19 N-(2,5-Difluoro-4-nitrophenyl)acetamide (26)

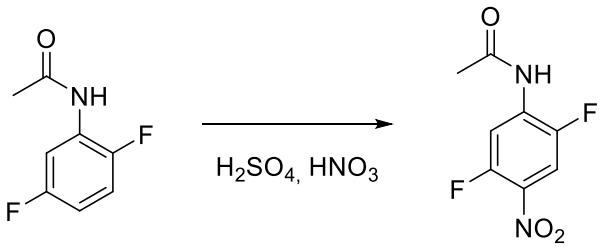

25 **26**

40 mL conc. sulfuric acid and 20 mL conc. nitric acid were cooled to 0 °C in a three-necked flask. **25** (1 eq, 15.5 mmol, 2.65 g) was added in small portions over 30 minutes. After stirring for about 2 h, the reaction mixture was poured on ice water and stirred for another hour. The precipitate was filtered off, washed with H_2O and dried under reduced pressure to give **26** (2.56 g, 11.8 mmol, 77%).

^{1}H NMR (400 MHz, $CDCl_3$, FID BIM188/10) δ = 8.54 (dd, J = 13.0, 6.5 Hz, 1H), 7.91 (dd, J = 10.5, 6.6 Hz, 1H), 7.59 (s, 1H), 2.30 (s, 3H) ppm.

D.4.1.20 1,4-Difluoro-2,5-dinitrobenzene (27)

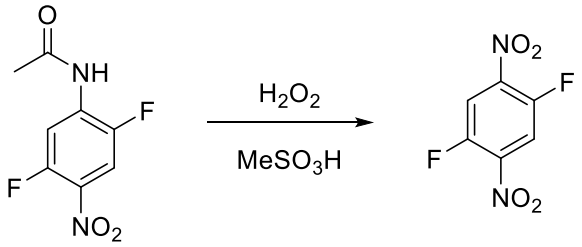

26 **27**

26 (1 eq, 5.9 mmol, 1.27 g) was dissolved in 20 mL methanesulfonic acid, 6 mL H_2O_2 were added dropwise and the reaction mixture was heated to 55 °C for 5 h. After cooling to room temperature, the solution was poured onto ice. The yellow precipitate was filtered off and washed with H_2O to give **27** (775 mg, 3.8 mmol, 64%) as yellow solid.

^{1}H NMR (400 MHz, $CDCl_3$, FID BIM192/10) δ = 8.06 (t, J = 7.5 Hz, 2H) ppm.

D.4.2 Synthesis of Alkyne-linked 5NICz

D.4.2.1 2-Bromopyrido[3',4':4,5]pyrrolo[3,2,1-jk]carbazole (XIV)

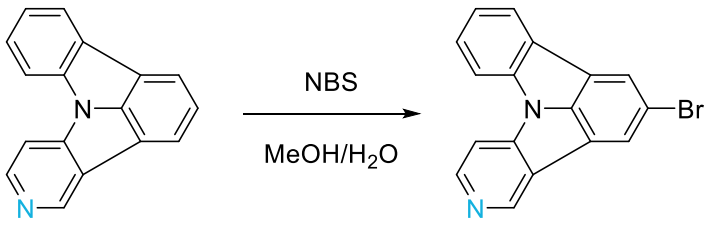

28 **XIV**

5NICz **28** (1 eq, 5.7 mmol, 1.369 g) was dissolved in 113 mL MeOH/H_2O (30%) and heated to 55 °C. NBS (1.05 eq, 6 mmol, 1.072 g) was added in small portion over a period of 24 h and then stirred for 23 h. After cooling to room temperature, the suspension was poured on 2N NaOH and stirred for one hour. The resulting off-white solid was filtered off, washed with H_2O and dried under reduced pressure. The crude product was refluxed in ACN, filtered off and dried. Recrystallization from toluene yielded **XIV** (775 mg, 2.4 mmol, 43%) as off-white solid.

^{1}H NMR (400 MHz, $CDCl_3$, FID BIM139/60) δ = 9.24 (d, J = 1.1 Hz, 1H), 8.71 (dd, J = 5.7, 1.4 Hz, 1H), 8.09 (dt, J = 9.5, 1.4 Hz, 2H), 8.04 – 7.98 (m, 1H), 7.81 (dd, J = 7.9, 1.0 Hz, 1H), 7.70 (dt, J = 5.6, 1.3 Hz, 1H), 7.59 (td, J = 7.7, 1.3 Hz, 1H), 7.41 (td, J = 7.6, 1.1 Hz, 1H) ppm.

^{13}C NMR (101 MHz, $CDCl_3$, FID BIM139/71) δ = 147.4, 144.9, 142.7, 141.7, 138.4, 129.7, 127.9, 125.2, 123.6, 123.4, 123.2, 122.8, 119.8, 117.2, 117.0, 112.9, 107.6 ppm.

D.4.2.2 2,2'-(1,2-Ethynediyl)pyrido[3',4':4,5]pyrrolo[3,2,1-jk]carbazole (XV)

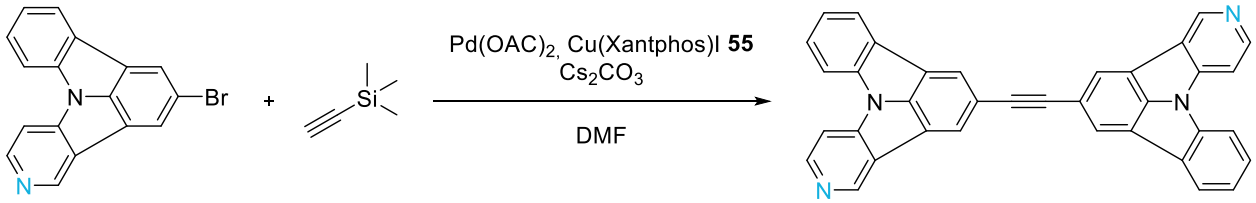

XIV **29** **XV**

Synthesis of **XV** was done following the procedure of Qiu et al.[26]

Bromo-5NICz **XIV** (1 eq, 1.2 mmol, 386 mg), TMS-acetylene **29** (0.6 eq, 0.7 mmol, 71 mg), $Pd(OAc)_2$ (0.01 eq, 0.012 mmol, 3 mg), Cu(Xantphos)I **55** (0.01 eq, 0.012 mmol, 10 mg) and Cs_2CO_3 (2 eq, 2.4 mmol, 793 mg) were suspended in 3.6 mL DMF under argon atmosphere and heated to 60 °C for 24 h. After cooling to room temperature, the solvent was evaporated under reduced pressure. The residue was stirred in a mixture of H_2O and ethyl acetate for 10 min, filtrated and dried to give **XV** (222 mg, 0.4 mmol, 73%) crude as brown solid.

D.4.3 Synthesis of 5,11NICz Building Block for Target Molecule TM2

D.4.3.1 4,4'-Iminobis-(1-methyl)pyridiniumdiiodide (33)

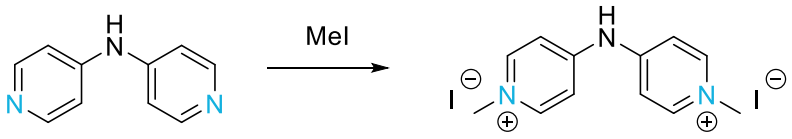

30 **33**

30 (1 eq, 2.92 mmol, 500 mg) was suspended in 12 mL MeI and stirred at room temperature for 24 h. The yellow solid was filtered and washed with DCM. As this yielded both the onefold reacted intermediate and the product, the yellow solid was again suspended in 12 mL MeI and stirred at room temperature for 48 h. The solid was filtered and washed with DCM to yield **33** (1.105 g, 2.4 mmol, 83%) as yellow solid.

^{1}H NMR (400 MHz, DMSO-d_6, FID BIM103/20) δ = 11.55 (s, 1H), 8.74 (d, *J* = 6.8 Hz, 4H), 7.78 (d, *J* = 6.8 Hz, 4H), 4.21 (s, 6H) ppm.

^{13}C NMR (101 MHz, DMSO-d6, FID BIM103/21) δ = 151.6, 146.0, 114.8, 46.2 ppm.

D.4.3.2 N-(2,6-Dichlorophenyl)-N-4-pyridinyl-4-pyridinamine (XVI)

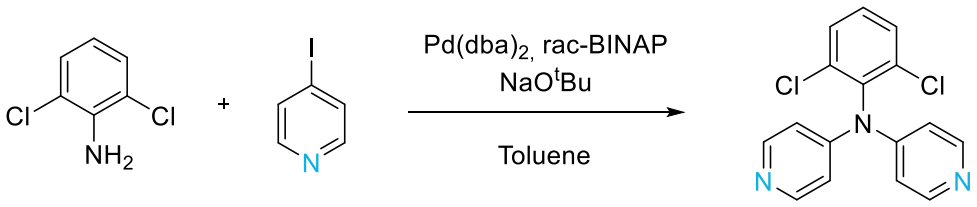

35 **36** **XVI**

35 (1 eq, 0.73 mmol, 118 mg), 4-iodopyridine **36** (2.7 eq, 1.97 mmol, 404 mg) and NaO^{t}Bu (4 eq, 2.9 mmol, 285 mg) were dissolved in 3 mL anhydrous, degassed toluene under argon atmosphere and light exclusion and heated to 110 °C. $Pd(dba)_2$ (0.2 eq, 0.15 mmol, 84 mg) and rac-BINAP (0.2 eq, 0.15 mmol, 93 mg) were added portion wise over ten days. After cooling to room temperature, the solution was poured onto H_2O and extracted with EE three times. The combined organic phases were washed with H_2O, dried over Na_2SO_4 and the solvent was evaporated under reduced pressure. The crude product was purified *via* column chromatography (99 g SG, DCM:MeOH 1%) twice to give **XVI** (10.5 mg, 0.03 mmol, 5%) as white solid.

^{1}H NMR (400 MHz, $CDCl_3$, FID BIM136/130) δ = 8.45 (dd, J = 6.25, 1.42 Hz, 4H), 7.53 – 7.47 (m, 2H), 7.38 (dd, J = 8.8, 7.4 Hz, 1H), 6.93 – 6.85 (dd, J = 6.37, 1.61 4H) ppm.

^{13}C NMR (101 MHz, $CDCl_3$, FID BIM136/31) δ = 151.0, 149.9, 137.5, 136.8, 130.6, 129.9, 114.6 ppm.

D.4.3.3 N-(2,6-Dichlorophenyl)-4-pyridinamine (XVIII)

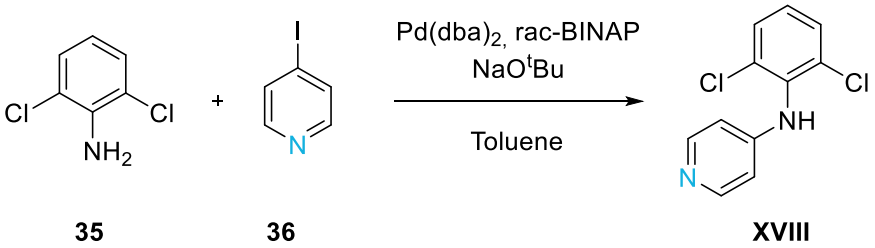

35 **36** **XVIII**

35 (1 eq, 0.7 mmol, 112 mg), 4-iodopyridin **36** (1 eq, 0.7 mmol, 140 mg), $Pd(dba)_2$ (0.04 eq, 0.03 mmol, 16 mg), rac-BINAP (0.04 eq, 0.03 mmol, 17 mg) and NaO^tBu (2 eq, 1.4 mmol, 139 mg) were dissolved in 3 mL anhydrous, degassed toluene under argon atmosphere and light exclusion and heated to 110 °C until full conversion (TLC, GC-MS). The reaction mixture was cooled to room temperature, poured on H_2O and extracted with EE three times. The combined organic layers were washed with H_2O, dried over Na_2SO_4 and the solvent was removed under reduced pressure. The crude product was purified *via* column chromatography (18 g SG, DCM:MeOH 1%) to give **XVIII** (123 mg, 0.51 mmol, 75%) as colorless crystalline solid.

^{1}H NMR (400 MHz, $CDCl_3$, FID BIM195/10) δ = 8.35 – 8.28 (m, 2H), 7.43 (d, J = 8.1 Hz, 2H), 7.19 (dd, J = 8.5, 7.7 Hz, 1H), 6.54 – 6.47 (m, 2H), 5.96 (s, 1H) ppm.

^{13}C NMR (101 MHz, $CDCl_3$, FID BIM195/11) δ = 150.3, 150.2, 134.2, 133.4, 129.1, 127.7, 109.8 ppm.

D.4.3.4 6-Chloro-5H-pyrido[4,3-b]indole (39)

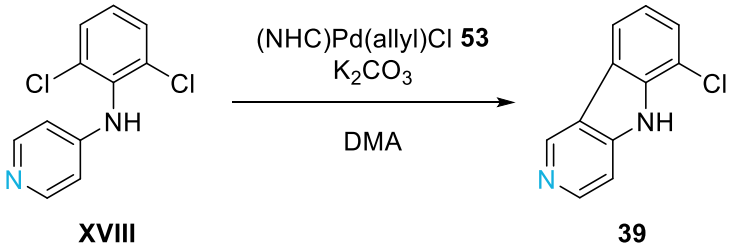

XVIII **39**

XVIII (1 eq, 1.6 mmol, 386 mg), (NHC)Pd(allyl)Cl **53** (0.05 eq, 0.08 mmol, 50 mg) and K_2CO_3 (2 eq, 3.2 mmol, 449 mg) were heated to 130 °C in 16 mL degassed DMA (with 1000 ppm H_2O) under argon atmosphere for eight days. The reaction mixture was cooled to room temperature, poured on H_2O and extracted with DCM three times. The combined organic layers were washed with H_2O, dried over Na_2SO_4 and the solvent was removed under reduced pressure. The crude product was purified *via* column chromatography (13 g SG, EE:MeOH 1%) to give **39** (52 mg, 0.26 mmol, 16%) as rose solid.

^{1}H NMR (400 MHz, DMSO-d6, FID BIM213/50) δ = 12.04 (s, 1H), 9.38 (s, 1H), 8.48 (d, J = 5.7 Hz, 1H), 8.23 (dd, J = 7.8, 1.0 Hz, 1H), 7.57 (dd, J = 7.8, 1.0 Hz, 1H), 7.51 (dd, J = 5.7, 1.1 Hz, 1H), 7.28 (t, J = 7.8 Hz, 1H) ppm.

D.4.4 Synthesis of NICz Building Block for Target Molecule TM3

D.4.4.1 N-2-Pyridinyl-2-pyridinamine (42)

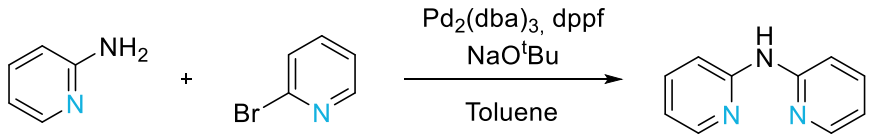

40 **41** **42**

40 (1 eq, 2 mmol, 188 mg), $Pd_2(dba)_3$ (0.02 eq, 0.04 mmol, 37 mg), dppf (0.04 eq, 0.08 mmol, 44 mg), NaO*t*Bu (1.4 eq, 2.8 mmol, 270 mg) and 12 mL anhydrous, degassed toluene were placed in a three-necked flask under argon atmosphere with reflux condenser. **41** (1.2 eq, 2.4 mmol, 0.24 mL) was added in argon counterflow and the reaction was heated to 110 °C for 36 h. The brown suspension was filtered over celite, washed with EE and the solvent was evaporated under reduced pressure. The crude product was purified *via* flash chromatography (49 g SG, DCM:MeOH 1 → 4%) to yield **42** (271 g, 1.6 mmol, 79%) as rose solid.

^{1}H NMR (400 MHz, CD_2Cl_2, FID BIM108/60) δ = 8.24 (ddd, J = 5.0, 1.9, 1.0 Hz, 2H), 7.66 – 7.54 (m, 4H), 7.50 (s, 1H), 6.85 (ddd, J = 6.6, 5.0, 1.4 Hz, 2H) ppm.

D.4.4.2 N-(2,6-Dichlorphenyl)-N-2-pyridinyl-2-pyridinamine (XXII)

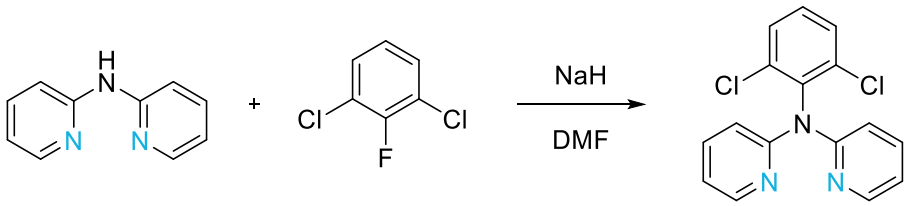

42 **34** **XXII**

42 (1 eq, 0.8 mmol, 137 mg) was dissolved in 1.6 mL DMF under argon atmosphere. NaH (2 eq, 1.6 mmol, 53 mg) was added to the reaction mixture. The reaction was stirred for 1 h at 40 °C, before **34** (1.5 eq, 1.2 mmol, 198 mg) was added via syringe. After stirring for 17 h at 50 °C, another equivalent of NaH (2 eq, 1.6 mmol, 53 mg) was added and the reaction was heated to 130 °C. After eight days the reaction was cooled to room temperature, poured onto H_2O and extracted with DCM three times. The combined organic layers were washed with H_2O, dried over Na_2SO_4 and the solvent was removed under reduced pressure. The crude product was purified *via* flash chromatography (DCM:MeOH 1%) to give **XXII** (15.8 mg, 0.05 mmol, 6%) as brown crystals.

^{1}H NMR (400 MHz, $CDCl_3$, FID BIM110/20) δ = 8.29 (ddd, J = 5.0, 2.0, 0.9 Hz, 2H), 7.58 (ddd, J = 8.3, 7.3, 2.0 Hz, 2H), 7.46 (d, J = 7.9 Hz, 2H), 7.29 – 7.24 (m, 1H), 7.11 (dt, J = 8.4, 0.9 Hz, 2H), 6.92 (ddd, J = 7.3, 4.9, 1.0 Hz, 2H) ppm.

D.4.4.3 N-(2,6-Dichlorophenyl)-N-2-pyridinyl-2-pyridinamine (XXII)

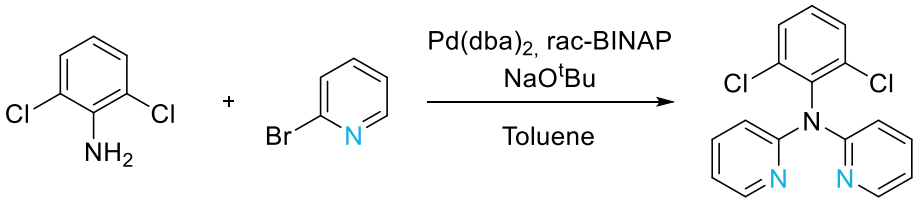

35 **41** **XXII**

35 (1 eq, 0.25 mmol, 43 mg), **41** (3 eq, 0.75 mmol, 119 mg), $Pd(dba)_2$ (0.04 eq, 0.01 mmol, 7 mg), rac-BINAP (0.04 eq, 0.01 mmol, 9 mg) and NaO^tBu (4 eq, 1 mmol, 98 mg) were dissolved in 1 mL anhydrous, degassed toluene and stirred 24 h at 110 °C under argon atmosphere. After cooling to room temperature, the solution was poured on H_2O and extracted with EE three times. The combined organic layers were washed with H_2O, dried over Na_2SO_4 and the solvent was removed under reduced pressure. The crude product was purified *via* column chromatography (13 g SG, DCM:MeOH 0.1 → 1%) and recrystallization from EtOH yielded **XXII** (49 mg, 0.16 mmol, 63%) as brown crystals.

^{1}H NMR (400 MHz, $CDCl_3$, FID BIM120/50) δ = 8.31 (ddd, J = 4.9, 2.0, 0.9 Hz, 2H), 7.60 (ddd, J = 8.4, 7.2, 2.0 Hz, 2H), 7.49 – 7.43 (m, 2H), 7.31 – 7.27 (m, 1H), 7.13 (dt, J = 8.4, 1.0 Hz, 2H), 6.93 (ddd, J = 7.3, 4.9, 1.0 Hz, 2H) ppm.

^{13}C NMR (101 MHz, $CDCl_3$, FID BIM120/51) δ = 155.7, 148.3, 139.4, 137.5, 136.6, 129.3, 129.0, 118.0, 114.6 ppm.

D.4.4.4 1-(2-Pyridinyl)-1H-benzotriazole (45)

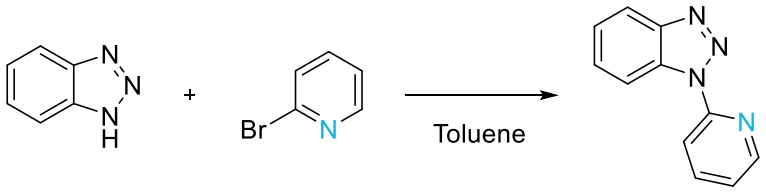

1 **41** **45**

45 was synthesized following the procedure of Xu et al.[19]

1 (2 eq, 294 mmol, 35 g) was suspended in 150 mL toluene under argon atmosphere and **41** (1 eq, 147 mmol, 23.8 g) was added under argon counterflow. The reaction mixture was heated to reflux until full conversion (TLC), cooled to room temperature and diluted with 2N NaOH and EE. The aqueous layer was extracted with EE three times and the combined organic layers were washed with H_2O. After drying over Na_2SO_4, the solvent was removed under reduced pressure to give **45** (15.3 g, 78 mmol, 52%) as off-white solid.

^{1}H NMR (400 MHz, $CDCl_3$, FID BIM215/10) δ = 8.67 (dt, J = 8.4, 1.0 Hz, 1H), 8.62 (ddd, J = 4.9, 1.9, 0.9 Hz, 1H), 8.31 (dt, J = 8.3, 1.0 Hz, 1H), 8.13 (dt, J = 8.3, 1.0 Hz, 1H), 7.95 (ddd, J = 8.4, 7.4, 1.9 Hz, 1H), 7.61 (ddd, J = 8.3, 7.0, 1.1 Hz, 1H), 7.46 (ddd, J = 8.2, 7.0, 1.1 Hz, 1H), 7.36 – 7.31 (m, 1H) ppm.

D.4.4.5 9H-Pyrido[2,3-b]indole (46)

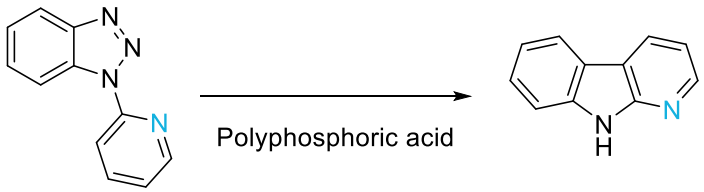

45 **46**

Synthesis of **46** was done according to Robinson and Thornley.[20]

45 (1 eq, 51 mmol, 10 g) and polyphosphoric acid (16 eq, 815 mmol, 80 g) were heated to 140 °C in a three-necked flask for about 8 h. After cooling to room temperature, the reaction mixture was diluted with H_2O and the brown precipitate was filtered off. 4N NaOH was added to the filtrate to give basic conditions. The yellow solid was filtered off, washed with H_2O and dried under reduced pressure. The crude product was recrystallized from toluene to give **46** (2.15 g, 12.7 mmol, 25%) as off-white needles.

^{1}H NMR (400 MHz, DMSO-d6, FID BIM223/20) δ = 11.77 (s, 1H), 8.50 (ddd, J = 7.7, 1.6, 0.6 Hz, 1H), 8.41 (dd, J = 4.9, 1.6 Hz, 1H), 8.15 (d, J = 7.67 Hz, 1H), 7.53 – 7.40 (m, 2H), 7.26 – 7.16 (m, 2H) ppm.

D.4.4.6 9-(2-(3-Chloropyridinyl))-9H-pyrido[2,3-b]indole (XXIII)

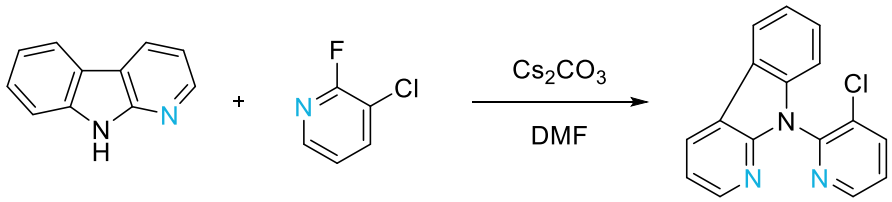

46 **47** **XXIII**

46 (1 eq, 1 mmol, 170 mg), **47** (1.2 eq, 1.2 mmol, 158 mg) and Cs_2CO_3 (1.2 eq, 1.2 mmol, 391 mg) were dissolved in 2 mL DMF under argon atmosphere and stirred at 130 °C until full conversion (TLC, GC-MS). The reaction mixture was cooled to room temperature, poured on H_2O and extracted with DCM three times. The combined organic layers were dried over Na_2SO_4, filtered and the solvent was evaporated under reduced pressure. The crude product was purified *via* column chromatography (49 g SG, PE:EE 50%) to give **XXIII** (247 mg, 0.88 mmol, 88%) as off-white solid.

^{1}H NMR (400 MHz, $CDCl_3$, FID BIM143/40) δ = 8.67 (dd, J = 4.7, 1.7 Hz, 1H), 8.48 (dd, J = 4.9, 1.6 Hz, 1H), 8.39 (dd, J = 7.7, 1.6 Hz, 1H), 8.12 (dt, J = 7.8, 1.0 Hz, 1H), 8.04 (dd, J = 8.1, 1.7 Hz, 1H), 7.51 – 7.42 (m, 2H), 7.35 (td, J = 7.5, 1.0 Hz, 1H), 7.29 – 7.22 (m, 2H) ppm.

^{13}C NMR (101 MHz, $CDCl_3$, FID BIM143/41) δ = 151.8, 148.1, 147.5, 146.5, 139.9, 139.3, 130.9, 128.6, 127.2, 124.8, 121.5, 121.4, 121.1, 116.9, 116.7, 111.0 ppm.

D.4.4.7 1-Methyl-2-(N-(2,6-dichlorophenyl)-N-(2-pyridinyl)amino)pyridiniumiodide (XXIV)

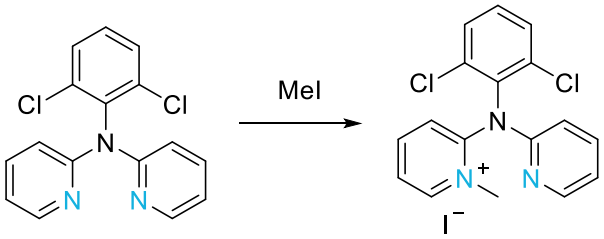

XXII **XXIV**

Synthesis of **XXIV** was done according to the procedure of Bures et at.[28]

XXII (1 eq, 0.3 mmol, 100 mg) was stirred in 3 mL MeI for seven days at room temperature. The solid was filtered off and dried under reduced pressure to give **XXIV** (92 mg, 0.2 mmol, 64%) as yellow solid.

^{1}H NMR (400 MHz, CDCl3, FID BIM170/10) δ = 9.98 (dd, J = 6.5, 1.7 Hz, 1H), 8.39 – 8.27 (m, 2H), 7.89 (ddd, J = 7.7, 6.3, 1.5 Hz, 1H), 7.75 (td, J = 7.8, 1.8 Hz, 1H), 7.61 – 7.53 (m, 2H), 7.47 (ddd, J = 8.7, 7.3, 1.4 Hz, 1H), 7.36 (dd, J = 8.4, 1.5 Hz, 1H), 7.20 – 7.13 (m, 1H), 6.66 (d, J = 8.2 Hz, 1H), 4.30 (d, J = 1.4 Hz, 3H) ppm.

D.4.4.8 Di-μ-chlorodichlorobis[N-2,6-dichlorophenyl)-N-2-pyridinyl-κN-2-pyridineamine-κN^{1}]dicopper (XXV)

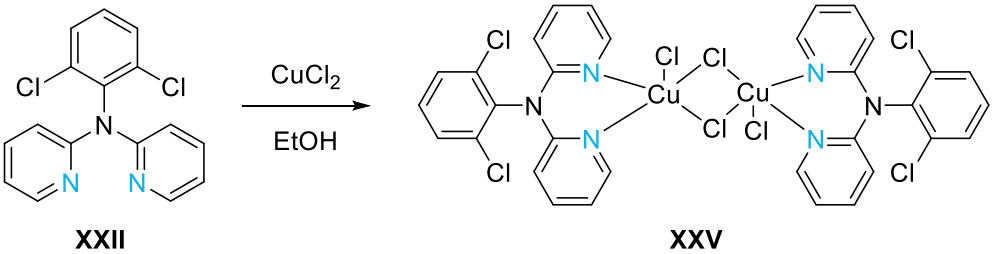

XXII **XXV**

XXII (1 eq, 1 mmol, 316 mg) and $CuCl_2$ (1.2 eq, 1.2 mmol, 162 mg) were dissolved in 10 mL EtOH and the reaction mixture was heated to reflux for 3 h. After cooling to room temperature, the solid was filtrated and dried to yield **XXV** (405 mg, 0.45 mmol, 90%) as green solid.

^{1}H NMR (400 MHz, DMSO-d6, FID BIM123/30) δ = 8.20 (s, 4H), 7.94 – 7.36 (m, 10H), 7.34 – 6.80 (m, 8H) ppm.

D.4.4.9 Dichloro[9-(2-(3-Chloropyridinyl-κN))-9H-pyrido-κN¹-[2,3-b]indole]copper (XXVI)

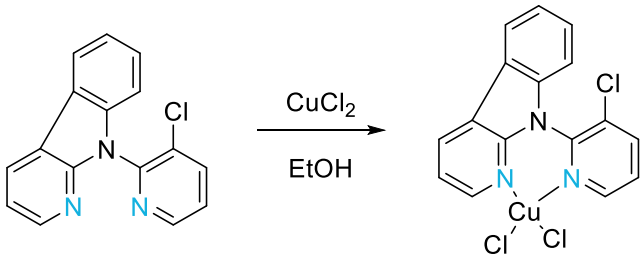

XXIII **XXVI**

XXIII (1 eq, 0.5 mmol, 136 mg) and $CuCl_2$ (1.2 eq, 0.6 mmol, 78 mg) were dissolved in 5 mL EtOH and the reaction mixture was heated to reflux for 48 h. After cooling to room temperature, the solid was filtered off, washed with EtOH and dried under reduced pressure. The crude product was recrystallized from ACN to give **XXVI** (75 mg, 0.18 mmol, 37%) as brown crystals.

^{1}H NMR (400 MHz, DMSO-d6, FID BIM151/10) δ = 8.71 (d, J = 4.6 Hz, 1H), 8.66 (d, J = 7.7 Hz, 1H), 8.40 (s, 1H), 8.32 (dd, J = 16.4, 7.9 Hz, 2H), 7.72 (dd, J = 8.2, 4.5 Hz, 1H), 7.49 (t, J = 7.7 Hz, 1H), 7.41 – 7.33 (m, 2H), 7.22 (d, J = 8.1 Hz, 1H) ppm.

D.4.4.10 9-(3-Nitro-2-pyridinyl)-9H-pyrido[2,3-b]indole (50)

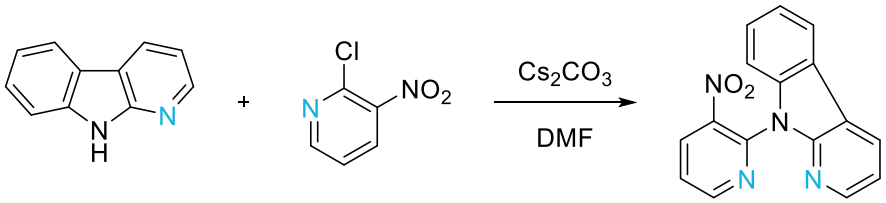

46 **49** **50**

The synthesis of **50** was done according to a modified procedure of Wharton et al.[33]

46 (1 eq, 0.7 mmol, 117 mg), **49** (1.2 eq, 0.8 mmol, 135 mg) and Cs_2CO_3 (1.2 eq, 0.8 mmol, 280 mg) were suspended in 1.4 mL DMF under argon atmosphere and heated to 130 °C until full conversion (TLC). The reaction mixture was poured on H_2O and extracted with DCM three times. Brine was added to the aqueous phase for better phase separation. The combined organic layers were washed with H_2O, dried over Na_2SO_4 and the solvent was removed under reduced pressure. The crude product was purified *via* column chromatography (DCM:MeOH 1%) to give **50** (89.3 mg, 0.3 mmol, 44%) as yellow solid.

^{1}H NMR (400 MHz, DMSO-d6, FID BIM187/10) δ = 9.02 (dd, J = 4.8, 1.6 Hz, 1H), 8.77 (dd, J = 8.2, 1.7 Hz, 1H), 8.66 (dd, J = 7.7, 1.6 Hz, 1H), 8.35 – 8.28 (m, 2H), 7.90 – 7.82 (m, 2H), 7.58 (ddd, J = 8.4, 7.3, 1.3 Hz, 1H), 7.45 (ddd, J = 8.1, 7.3, 1.0 Hz, 1H), 7.39 (dd, J = 7.7, 4.9 Hz, 1H) ppm.

D.4.4.11 2-(9H-Pyrido[2,3-b]indol-9-yl)-3-pyridinamine (XXVII)

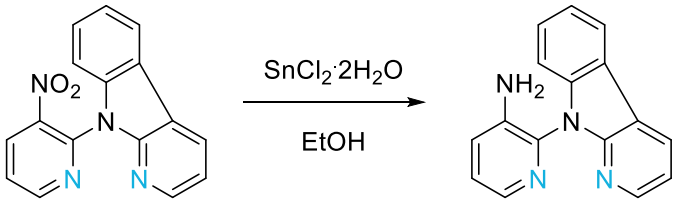

50 **XXVII**

XXVII was synthesized according to Dunlop and Tucker.[24]

50 (1 eq, 2.2 mmol, 644 mg) and $SnCl_2 \cdot 2H_2O$ (3.5 eq, 7.8 mmol, 1.75 g) were heated to reflux in 10 mL EtOH and stirred until full conversion (TLC, GC-MS). The reaction mixture was cooled to room temperature and poured onto water. 2N NaOH was added to give basic conditions. The aqueous solution was extracted with DCM. Brine was added to the aqueous phase for better phase separation. The combined organic layers were washed with H_2O, dried over Na_2SO_4 and the solvent was removed under reduced pressure to give **XXVII** (578 mg, 2.2 mmol, quant.) as grey solid.

^{1}H NMR (400 MHz, $CDCl_3$, FID BIM196/10) δ = 8.48 (dd, J = 4.9, 1.6 Hz, 1H), 8.40 (dd, J = 7.7, 1.6 Hz, 1H), 8.15 (dd, J = 4.6, 1.7 Hz, 1H), 8.11 (dt, J = 7.7, 1.0 Hz, 1H), 7.48 (ddd, J = 8.3, 7.1, 1.2 Hz, 1H), 7.41 (dt, J = 8.3, 1.0 Hz, 1H), 7.37 – 7.31 (m, 2H), 7.30 – 7.23 (m, 2H), 4.03 (s, 2H) ppm.

^{13}C NMR (101 MHz, $CDCl_3$, FID BIM196/11) δ = 151.5, 146.4, 139.7, 139.6, 137.1, 128.8, 127.4, 125.6, 124.5, 121.6, 121.3, 121.0, 117.3, 116.4, 111.9 ppm.

D.4.4.12 Pyrido[2,3-b]pyrido[3',2':4,5]pyrrolo[3,2,1-hi]indole (44)

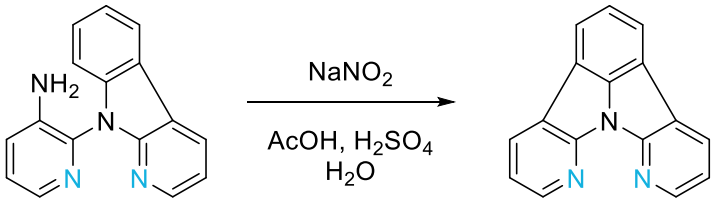

XXVII **44**

XXVII (1 eq, 4.1 mmol, 1.07 g) was dissolved in 10 mL acetic acid and cooled to 0 °C in an ice bath. After addition of 2.3 mL conc. sulfuric acid, where the temperature was kept below 40 °C, the reaction mixture was stirred for 1 h at room temperature. $NaNO_2$ (1.1 eq, 4.5 mmol, 312 mg) was dissolved in 6.6 mL H_2O and added dropwise to the cooled solution while keeping the temperature below 7 °C. After addition the reaction was heated to 90 °C for six days. The reaction mixture was cooled to room temperature, poured on a 2N NaOH solution and extracted with DCM six times. The combined organic layers were washed with H_2O, dried over Na_2SO_4, filtrated and the solvent was

removed under reduced pressure. The crude product was purified *via* column chromatography (49 g SG, LP/EE 20 → 80%) to yield **44** (8 mg, 0.03 mmol, 1%) as yellow solid.

^{1}H NMR (400 MHz, $CDCl_3$, FID BIM210/60) δ = 8.65 (dd, J = 5.0, 1.6 Hz, 2H), 8.39 (dd, J = 7.7, 1.7 Hz, 2H), 8.07 (d, J = 7.5 Hz, 2H), 7.64 (t, J = 7.5 Hz, 1H), 7.34 (dd, J = 7.8, 5.0 Hz, 2H) ppm.

^{13}C NMR (101 MHz, $CDCl_3$, FID BIM210/63) δ = 150.5, 147.0, 142.0, 131.0, 124.0, 123.9, 121.0, 118.2, 116.7 ppm.

D.4.5 Synthesis of Catalysts

D.4.5.1 [1,3-Bis[2,6-bis(1-methylethyl)phenyl]-1,3-dihydro-2H-imidazol-2-yliden]chloro(η³-2-propen-1-yl)palladium (53)

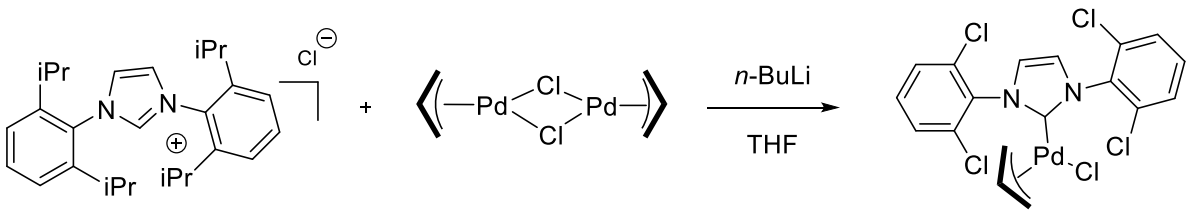

51 **52** **53**

51 (5 eq, 38.75 mmol, 3.72 g) was dissolved in 53 mL anhydrous THF in a three-necked flask under argon atmosphere and *n*-BuLi (5.1 eq, 8.9 mmol, 2.5 M, 3.57 mL) was slowly added at room temperature. After 45 minutes **52** (1 eq, 1.75 mmol, 0.67 g) was added and the reaction mixture was stirred for 3 h at room temperature. The solution was filtered over celite and the solvent was removed under reduced pressure. Purification *via* flash chromatography (180 g SG, DCM:Et_2O 0 → 3%) yielded **53** (1.81 g, 3.2 mmol, 89%) as yellow solid.

^{1}H NMR (400 MHz, $CDCl_3$, FID BIM135/10) δ = 7.42 (t, J = 7.7 Hz, 2H), 7.30 – 7.26 (m, 5H), 7.15 (s, 2H), 4.81 (tt, J = 13.5, 7.2 Hz, 1H), 3.90 (dd, J = 7.5, 2.1 Hz, 1H), 3.16 – 3.02 (m, 3H), 2.89 – 2.75 (m, 3H), 1.36 (dd, J = 22.4, 6.7 Hz, 12H), 1.17 (d, J = 6.8 Hz, 6H), 1.08 (d, J = 6.9 Hz, 6H) ppm.

D.4.5.2 Iodo[1,1'-(9,9-dimethyl-9H-xanthene-4,5-diyl)bis(1,1-diphenylphosphine-P)]copper(I) (55)

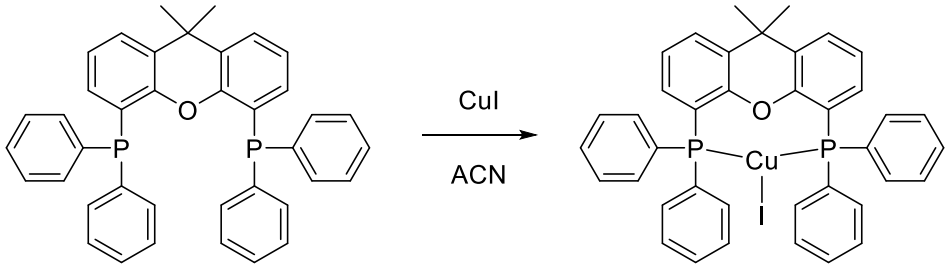

54 **55**

55 was synthesized according to the procedure of Huang et al.[27]

CuI (1 eq, 0.26 mmol, 50 mg) was dissolved in 3 mL anhydrous ACN at 50 °C. **54** (1.1 eq, 0.3 mmol, 166 mg) was added and the suspension was stirred at 50 °C overnight. After cooling to room temperature, the solid was filtered off, washed with ACN and dried to yield **55** (150 mg, 0.2 mmol, 75%) as white solid.

^{1}H NMR (400 MHz, CD_2Cl_2, FID BIM146/10) δ = 7.58 (dd, J = 7.8, 1.5 Hz, 2H), 7.45 – 7.39 (m, 8H), 7.35 (t, J = 7.4 Hz, 4H), 7.29 – 7.23 (m, 8H), 7.13 (t, J = 7.7 Hz, 2H), 6.61 (qd, J = 4.6, 1.5 Hz, 2H), 1.67 (s, 6H) ppm.

E. Bibliography

[1] S. R. Forrest, *Nature* **2004**, *428*, 911-918.

[2] J. Huang, J.-H. Su, H. Tian, *Journal of Materials Chemistry* **2012**, *22*, 10977-10989.

[3] Y. Shirota, H. Kageyama, *Chemical Reviews* **2007**, *107*, 953-1010.

[4] J. Mei, Y. Diao, A. L. Appleton, L. Fang, Z. Bao, *Journal of the American Chemical Society* **2013**, *135*, 6724-6746.

[5] L. Lan, J. Zou, C. Jiang, B. Liu, L. Wang, J. Peng, *Frontiers of Optoelectronics* **2017**, *10*, 329-352.

[6] A. P. Kulkarni, C. J. Tonzola, A. Babel, S. A. Jenekhe, *Chemistry of Materials* **2004**, *16*, 4556-4573.

[7] M. A. Baldo, D. F. O'Brien, Y. You, A. Shoustikov, S. Sibley, M. E. Thompson, S. R. Forrest, *Nature* **1998**, *395*, 151-154.

[8] T. Chatterjee, K.-T. Wong, *Advanced Optical Materials* **2019**, *7*, 1800565.

[9] A. Endo, K. Sato, K. Yoshimura, T. Kai, A. Kawada, H. Miyazaki, C. Adachi, *Applied Physics Letters* **2011**, *98*, 083302.

[10] Y. Liu, C. Li, Z. Ren, S. Yan, M. R. Bryce, *Nature Reviews Materials* **2018**, *3*, 18020.

[11] M. Y. Wong, E. Zysman-Colman, *Advanced Materials* **2017**, *29*, 1605444.

[12] Y.-H. Niu, Y.-L. Tung, Y. Chi, C.-F. Shu, J. Kim, B. Chen, J. Luo, A. Carty, A. Jen, *Chemistry of Materials,* **2005**, *17*.

[13] B. Mi, Z. Gao, Z. Liao, W. Huang, C. H. Chen, *Science China Chemistry* **2010**, *53*, 1679-1694.

[14] P. Kautny, D. Lumpi, Y. Wang, A. Tissot, J. Bintinger, E. Horkel, B. Stöger, C. Hametner, H. Hagemann, D. Ma, J. Fröhlich, *Journal of Materials Chemistry C* **2014**, *2*, 2069-2081.

[15] M.-H. Tsai, H.-W. Lin, H.-C. Su, T.-H. Ke, C.-c. Wu, F.-C. Fang, Y.-L. Liao, K.-T. Wong, C.-I. Wu, *Advanced Materials* **2006**, *18*, 1216-1220.

[16] Y. Tao, C. Yang, J. Qin, *Chemical Society Reviews* **2011**, *40*, 2943-2970.

[17] T. Kader, B. Stöger, J. Fröhlich, P. Kautny, *Chemistry – A European Journal* **2019**, *25*, 4412-4425.

[18] X. Zhang, H. Dong, W. Hu, *Advanced Materials* **2018**, *30*, 1801048.

[19] K. Xu, N. Thieme, B. Breit, *Angewandte Chemie* **2014**, *126*, 7396-7399.

[20] R. Robinson, S. Thornley, *Journal of the Chemical Society, Transactions* **1924**, *125*, 2169-2176.

[21] N. Marion, O. Navarro, J. Mei, E. D. Stevens, N. M. Scott, S. P. Nolan, *Journal of the American Chemical Society* **2006**, *128*, 4101-4111.

[22] H. W. H. Lai, Y. C. Teo, Y. Xia, *ACS Macro Letters* **2017**, *6*, 1357-1361.

[23] W. W. Porter, T. P. Vaid, A. L. Rheingold, *Journal of the American Chemical Society* **2005**, *127*, 16559-16566.

[24] H. G. Dunlop, S. H. Tucker, *Journal of the Chemical Society (Resumed)* **1939**, 1945-1956.

[25] V. Fagan, S. Bonham, P. McArdle, M. P. Carty, F. Aldabbagh, *European Journal of Organic Chemistry* **2012**, *2012*, 1967-1975.

[26] S. Qiu, C. Zhang, R. Qiu, G. Yin, J. Huang, *Advanced Synthesis & Catalysis* **2018**, *360*, 313-321.

[27] J. Huang, J. Chan, Y. Chen, C. J. Borths, K. D. Baucom, R. D. Larsen, M. M. Faul, *Journal of the American Chemical Society* **2010**, *132*, 3674-3675.

[28] F. Bureš, D. Cvejn, K. Melánová, L. Beneš, J. Svoboda, V. Zima, O. Pytela, T. Mikysek, Z. Růžičková, I. V. Kityk, A. Wojciechowski, N. AlZayed, *Journal of Materials Chemistry C* **2016**, *4*, 468-478.

[29] Y. Koga, T. Kaneda, Y. Saito, K. Murakami, K. Itami, *Science* **2018**, *359*, 435-439.

[30] M. Daigle, A. Picard-Lafond, E. Soligo, J.-F. Morin, *Angewandte Chemie International Edition* **2016**, *55*, 2042-2047.

[31] Y. Choi, T. Chatterjee, J. Kim, J. S. Kim, E. J. Cho, *Organic & Biomolecular Chemistry* **2016**, *14*, 6804-6810.

[32] G. U. Chaturbhuj, K. G. Akamanchi, *Tetrahedron Letters* **2011**, *52*, 4950-4953.

[33] S. I. Wharton, J. B. Henry, H. McNab, A. R. Mount, *Chemistry – A European Journal* **2009**, *15*, 5482-5490.